

**Antibodies to myelin oligodendrocyte glycoprotein
(MOG): Analysis of the impact of the glycosylation site
of MOG for recognition of human autoantibodies and
dissection of effector functions of the anti-MOG
monoclonal antibody 8-18C5**

Dissertation zur Erlangung des Doktorgrades der
Naturwissenschaften (Dr. rer. nat.) der Fakultät für Biologie der
Ludwig-Maximilians-Universität München

Iris Martí Fernández

München, 2020

Diese Dissertation wurde angefertigt unter der Leitung von Prof.
Dr. Edgar Meinl am Institut für Klinische Neuroimmunologie
(Biomedizinisches Zentrum, Martinsried)

Erstgutachter: Prof. Dr. Wolfgang Enard

Zweitgutachter: Prof. Dr. Daniel Krappmann

Sondervotum: Prof. Dr. Edgar Meinl

Tag der Abgabe: 26.05.2020

Tag der mündliche Prüfung: 01.12.2020

ERKLÄRUNG

Hiermit versichere ich an Eides statt, dass meine Dissertation selbständig und ohne unerlaubte Hilfsmittel angefertigt worden ist.

Die vorliegende Dissertation wurde weder ganz, noch teilweise, bei einer anderen Prüfungskommission vorgelegt.

Ich habe noch zu keinem früheren Zeitpunkt versucht, eine Dissertation einzureichen oder an einer Doktorprüfung teilzunehmen.

München, der 22.12.2020

Iris Martí Fernández

Note on results obtained in collaboration:

Mass spectrometry experiments were performed and analysed by Dr. Paul Hensbergen, Agnes L. Hipgrave Ederveen and Dr. Manfred Wuhrer from the Center for Proteomics and Metabolomics, Leiden University Medical Center, Leiden, Netherlands.

Summary

Autoantibodies to myelin oligodendrocytes glycoprotein (MOG) are found in a proportion of patients with inflammatory demyelination and are detected with MOG-transfected cells. MOG is a transmembranous glycoprotein displayed on the outside of internodal myelin; its extracellular part forms an IgV-like fold. While the prototype anti-MOG mAb 8-18C5 and polyclonal anti-MOG responses from different mouse strains largely recognize the FG loop of MOG, the human anti-MOG response is more heterogeneous and human MOG-Abs recognizing different epitopes were found to be pathogenic.

The first aim of this thesis was to get further insight into details of antigen-recognition by human MOG-Abs focusing on the impact of glycosylation. MOG has one known N-glycosylation site at N31 located in the BC loop linking two beta-sheets. Reactivity towards wild-type MOG and two different aglycosylated was measured using a cell-based assay. Around 60 % of all patients (16/27) showed an altered reactivity to one or both of the mutations. 7 different patterns of recognition of the two glycosylation-deficient mutants by different patients were identified. In 7/27 patients the neutral glycosylation-deficient mutant was recognized stronger. The glycan structures of HEK- and myelin-derived MOG were determined by mass spectrometry.

Previous studies from the lab have shown that MOG antibodies from patients are pathogenic by two different effector mechanisms, namely demyelination and enhancement of the activation of MOG-specific T cells, but it is unknown which Fc effector functions, complement activation and FcγR-activation, are linked to which pathomechanisms.

The second part of this thesis is imbedded into the bigger aim to link these pathomechanisms to Fc-functions. To this end, the pathogenic mAb 8-18C5 is applied as a model system. A recombinant version of this mAb with a human IgG1 Fc part is used and 10 clones containing 12 different mutations in the Fc part were introduced. These mutations were selected based on previous publications with other recombinant mAbs. These mutated variants of the 8-18C5 were analysed for antigen-recognition, C1q-binding by ELISA, and FcγRIII activation with a reporter cell line. Thereby a panel of Fc variants of the anti-MOG mAb 8-18C5 was generated that differs with respect to C1q-binding and FcγRIII activation.

Together, this thesis showed the importance of the glycosylation site of MOG for binding of autoantibodies. The finding that the glycan provides a hindrance for antibody binding in a proportion of patients has implications for development of assays to enhance the sensitivity to detect antibodies to MOG and provided further insight into details of antigen-recognition and extended the known heterogeneity of human autoantibodies against MOG. Moreover, the 8-18C5 variants cloned in this project provide the basis for future in vivo transfer experiments to link Fc effector functions to different aspects of disease pathology triggered by MOG autoantibodies.

Zusammenfassung

Autoantikörper gegen Myelin Oligodendrozyten Glykoprotein (MOG) werden bei einer Subgruppe von Patienten mit entzündlicher Demyelinisierung gefunden und mit MOG-transfizierten Zellen detektiert. MOG ist ein transmembranes Glykoprotein, das auf der Außenseite des internodalen Myelin exprimiert wird; sein extrazellulärer Teil bildet eine Immunglobulin-artige Domäne. Während der Prototyp anti-MOG monoklonale Antikörper (mAk) Ab 8-18C5 und die polyklonalen anti-MOG Antikörper von verschiedenen Mäusestämmen vorwiegend die FG-Schleife von MOG erkennen, ist die menschliche anti-MOG Antwort heterogener und es wurde gefunden, dass menschliche MOG-Aks verschiedene Epitope erkennen und pathogen sind.

Das erste Ziel dieser Doktorarbeit war es, weiteren Einblick in Details der Antigenerkennung der menschlichen MOG-Aks zu erhalten und speziell die Rolle der Glykosylierung zu untersuchen. MOG hat eine bekannte N-Glykosylierungsstelle bei N31 in der BC-Schleife, die zwei *beta-sheets* verbindet. Die Reaktivität gegenüber Wildtyp MOG und zwei verschiedenen Glykosylierungs-defizienten Mutanten wurde unter Verwendung eines zellbasierten Assays gemessen. Diese Untersuchungen ergaben, dass etwa 60% aller Patienten mit MOG-Aks (16/27) eine veränderte Reaktivität gegenüber einer oder beiden Mutationen zeigten. 7 verschiedene Muster der Antigenerkennung der beiden Glykosylierungs-defizienten Mutanten von verschiedenen Patienten wurden identifiziert. In 7/27 Patienten wurde die neutrale Glykosylierungs-defiziente Mutante stärker erkannt. Die Glykanstrukturen von MOG von transfizierten HEK-Zellen von MOG aus Myelin wurden massenspektrometrisch bestimmt.

Frühere Studien aus dem Labor haben gezeigt, dass MOG-Antikörper von Patienten pathogen sind durch zwei verschiedene Effektomechanismen, nämlich Demyelinisierung und Verstärkung der Aktivierung von MOG-spezifischen T-Zellen. Es ist jedoch nicht bekannt welche Fc-Effektorfunktionen, Komplementaktivierung und FcγR-Aktivierung mit welchem Pathomechanismus zusammenhängen.

Der zweite Teil dieser Doktorarbeit wird in das größere Ziel eingebettet, herauszufinden, welche Pathomechanismen mit welchen Fc-Funktionen zusammenhängen. Zu diesem Zweck wird der pathogene mAb 8-18C5 als Modellsystem eingesetzt. Eine rekombinante Version dieses mAk mit einem humanen IgG1-FC Teil wird verwendet und 10 Klone mit 12 verschiedenen Mutationen im Fc-Teil wurden eingeführt. Diese Mutationen wurden basierend auf früheren Veröffentlichungen mit andern rekombinanten mAks ausgewählt. Diese mutierten Varianten des 8-18C5 wurden auf Antigenerkennung, C1q-Bindung

durch ELISA und FcγRIII-Aktivierung mit einer Reporterzelllinie analysiert. So konnte ein Panel an Varianten des anti-MOG mAbs 8-18C5 generiert werden, die sich hinsichtlich Bindung von C1q und Aktivierung von FcγRIII unterscheiden.

Zusammengefasst, diese Doktorarbeit zeigte die Bedeutung der Glykosylierungsstelle von MOG für die Bindung von Autoantikörpern. Der Befund, dass das Glycan die Antikörperbindung bei einem Teil der Patienten behindert, hat Auswirkungen auf die Entwicklung von Tests zur Erhöhung der Empfindlichkeit für den Nachweis von Antikörpern gegen MOG und lieferte weiter Einblicke in Einzelheiten der Antigenerkennung und erweiterte die bekannte Heterogenität menschlicher Autoantikörper gegen MOG. Darüber hinaus bilden die in diesem Projekt geklonten 8-18C5 Varianten die Grundlage für zukünftige Transferexperimente, um die Fc-Effektorfunktionen mit verschiedenen Aspekten der durch MOG-Autoantikörper ausgelösten Krankheitspathologie zu verknüpfen.

Acknowledgments

I would like to thank my supervisor Prof. Dr. Edgar Meinel for this interesting project. He not only generously shared his knowledge and was always there to answer to my questions, but also had faith in me and this project.

I am also grateful to my colleagues, who made going to work much more easily, especially Dr. Miriam Fichtner and Prof. Dr. Atay Vural.

I would also like to thank our collaborators, who performed the Mass spectrometry experiments, Dr. Paul Hensbergen, Agnes L. Hipgrave Ederveen and Dr. Manfred Wuhrer from the Center for Proteomics and Metabolomics, Leiden University Medical Center, Leiden, Netherlands.

Also, I would like to thank Dr. Stefanie Hauck and PD. Dr. Dieter Jenne for their valuable input and ideas which helped to further develop this project.

Finally, I would especially like to thank my family for their help and support all these years, without them I would not have made it this far.

Table of contents

Introduction

1. Inflammatory demyelinating diseases of the central nervous system (CNS).....	11
1.1 Role of B cells and antibodies.....	12
1.2 Therapeutic intervention targeting B cells and antibodies.....	13
2. Myelin oligodendrocyte glycoprotein (MOG).....	14
3. N-glycosylation and its role in antibody binding.....	15
4. MOG antibodies.....	16
4.1 MOG antibodies in patients and epitope mapping.....	16
5. Possible pathogenic mechanisms of MOG antibodies in humans.....	18
5.1 Complement activation and Fcγ receptor activation as effector mechanisms of antibodies.....	18
5.2 Role of Fc glycosylation.....	21

Objectives.....	22
------------------------	-----------

Materials and Methods

6. Materials.....	23
7. Methods.....	24
7.1 Mutagenesis.....	24
7.2 Transformation of competent bacterial cells by heat-shock.....	26
7.3 Plasmid preparation.....	26
7.4 Cell culture of HeLa cells.....	27
7.5 Cell culture of HEK 293 EBNA 1 cells.....	27
7.6 Cell culture of TE cells.....	27
7.7 Transfection of HeLa cells with jetPRIME.....	28
7.8 Transfection of HEK 293 EBNA 1 cells.....	28
7.9 Purification of recombinant protein by immobilized affinity chromatography (IMACS).....	28
7.10 Deglycosylation by PNGaseF.....	29
7.11 Determination of protein concentration.....	29
7.12 Sodium dodecyl sulfate polyacrylamide gel electrophoresis (SDS PAGE).....	29
7.13 Protein detection by Coomassie blue staining.....	30
7.14 Western blot.....	30
7.15 Enzymatic biotinylation of hMOG.....	30

7.16	Serum screening for MOG-Abs by FACS.....	31
7.17	Binding of recombinant 8-18C5 variants to hMOG.....	31
7.18	C1q binding of recombinant 8-18C5 variants.....	32
7.19	Purification of hMOG-EGFP from HeLa cells using His-tag dynabeads..	32
7.20	Purification of myelin glycoproteins from human and bovine brain with Lentil-lectin sepharose 4B column.....	33
7.21	ADCC activity of the 8-18C5 variants using murine FcγRIII effector cells.....	34
7.22	Preparation of ethyl esterified released N-glycans from recombinant MOG.....	34
7.23	MALDI-TOF(/TOF)-MS(/MS) analysis of released glycans.....	34
7.24	Statistics.....	35

Results

8.	MOG glycosylation site in autoantibody recognition and its glycan structures...36	
8.1	Characterization of the glycosylation deficient mutants.....	36
8.2	Heterogeneous response to two glycosylation deficient MOG mutants.....	37
8.3	Purification of MOG and myelin glycoproteins.....	41
8.4	Glycoforms of MOG.....	41
9.	Effector functions of wild-type mAb r8-18C5 and its variants.....	44
9.1	Characterization of the r8-18C5 mutants.....	45
9.2	Complement binding affinities of r8-18C5 variants.....	48
9.3	mFcγRIII activation by r8-18C5 variants.....	48

Discussion

10.	The glycosylation site of myelin oligodendrocytes glycoprotein affects autoantibody recognition in a large proportion of patients.....	51
11.	r8-18C5 variants and their effector functions.....	53

Conclusions.....	56
-------------------------	-----------

References.....	57
------------------------	-----------

List of abbreviations.....	65
-----------------------------------	-----------

Publication and Conferences.....	67
---	-----------

Introduction

1. Inflammatory demyelinating diseases of the central nervous system (CNS)

Inflammatory demyelinating diseases of the CNS comprise a broad spectrum of diseases including multiple sclerosis (MS), neuromyelitis optica spectrum disorders (NMOSD), optic neuritis (ON) and acute disseminated encephalomyelitis (ADEM) (Figure 1). MS is the most common chronic inflammatory disease of the CNS, it affects 1 in 1000 people in Western countries (Sadovnick and Ebers 1993). There are two major forms of MS: (1) 85-90% of the patients suffer from relapsing-remitting MS (RRMS), which is characterized by acute episodes of neurologic dysfunction, followed by periods of partial or complete remission with clinical stability between the relapses. After several years RRMS is followed by a secondary progressive MS (SPMS) phase in many patients, where there is an uninterrupted disease progression (Weinshenker et al. 1989). Some patients (10-15% of the cases) begin with primary progressive MS (PPMS) where there is disease progression from the onset (Kutzelnigg et al. 2005)

NMOSD is a rare disease with higher prevalence in Asia (Jacob et al. 2013). The principal characteristics that distinguish NMOSD from MS are its selective involvement of optic nerves and spinal cord, and its characteristic longitudinally extensive spinal cord lesions that are detected most sensitively by magnetic resonance imaging (MRI) (Weinshenker et al. 2006). Moreover, the detection of neuromyelitis optica immunoglobulin G (NMO-IgG), an autoantibody in the serum of patients with NMOSD against AQP4, distinguishes NMOSD from other demyelinating disorders (Wingerchuk et al. 2007)

ON is a common condition with higher incidence in Caucasians (1-5 in 100.000) and is characterized by a demyelinating inflammation of the optic nerve. It may be isolated or in association with MS or NMOSD. This condition usually presents a subacute unilateral loss of vision, although loss of vision in both eyes can also arise, either simultaneously or sequentially (Hickman et al. 2002).

ADEM occurs predominantly during early childhood and has often a monophasic course. It is an immune-mediated inflammatory disorder of the CNS, which is commonly preceded by an infection, and predominantly affects the white matter of the brain and spinal cord (Tenenbaum et al. 2007).

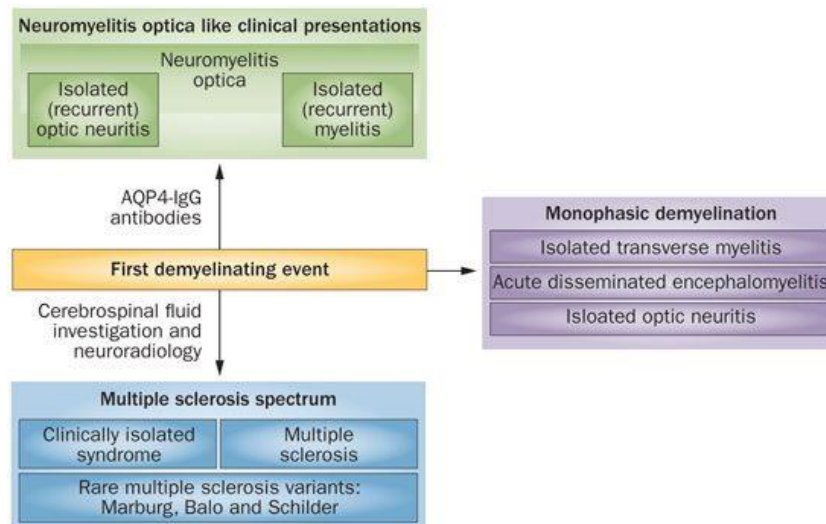


Figure 1: Acquired CNS inflammatory demyelinating diseases. Figure taken from (Reindl et al. 2013)

1.1 Role of B cells and antibodies

T cells can induce blood-brain barrier disruption and CNS inflammation; therefore, MS has been considered for many years as a T-cell driven disease. In addition to autoreactive T cells, there are several evidences suggesting that B cells and antibodies are also key players in inflammatory demyelinating diseases of the CNS.

Since it was first published, antibody production has become a diagnostic tool of neuroinflammatory disease (Kabat, Moore, and Landow 1942). Intrathecally produced antibodies can be visualized as oligoclonal bands (OCBs) in the cerebrospinal fluid (CSF) of MS patients (Obermeier et al. 2008). Together with the presence of clonally expanded B cells (CD138⁺ plasma cells) in the CSF (Von Büdingen et al. 2010) they indicate the existence of an antigen-driven B cell response.

Moreover, in a subset of MS patients deposition of IgG and activated complement can be observed in demyelinating areas of brain lesions (Lucchinetti et al. 2000) Active NMO lesions also show IgM deposition and complement activation (Lucchinetti et al. 2002; Misu et al. 2013). Furthermore, a large proportion of patients with MS type II pathology benefit from plasma exchange (Keegan et al. 2005) and B cell depleting therapies, such as anti-CD20 antibody (i.e. Rituximab), reduce the relapses in some MS and NMO patients (Hauser et al. 2008; Trebst et al. 2014).

Autoantibodies are relevant for the pathogenesis of demyelinating diseases of the CNS. Their importance was highlighted by the identification of IgG autoantibody (NMO-IgG) that localises in the blood-brain barrier and selectively binds to the water channel AQP4 on astrocytes. This serological marker is a valuable tool to distinguish NMO from MS

(Lennon et al. 2004; Lennon et al. 2005). Transfer studies in which human anti-AQP4 antibodies were injected into experimental autoimmune encephalomyelitis (EAE) mice, the animal model that closely resembles the clinical and pathological features of human MS, demonstrated the pathogenicity of these autoantibodies (Bennett et al. 2009; Bradl et al. 2009; Kinoshita et al. 2009).

In addition to their role to generate antibodies, B cells also perform a wide range of functions which are crucial for the pathogenesis of MS and related CNS disorders. (Figure 2)

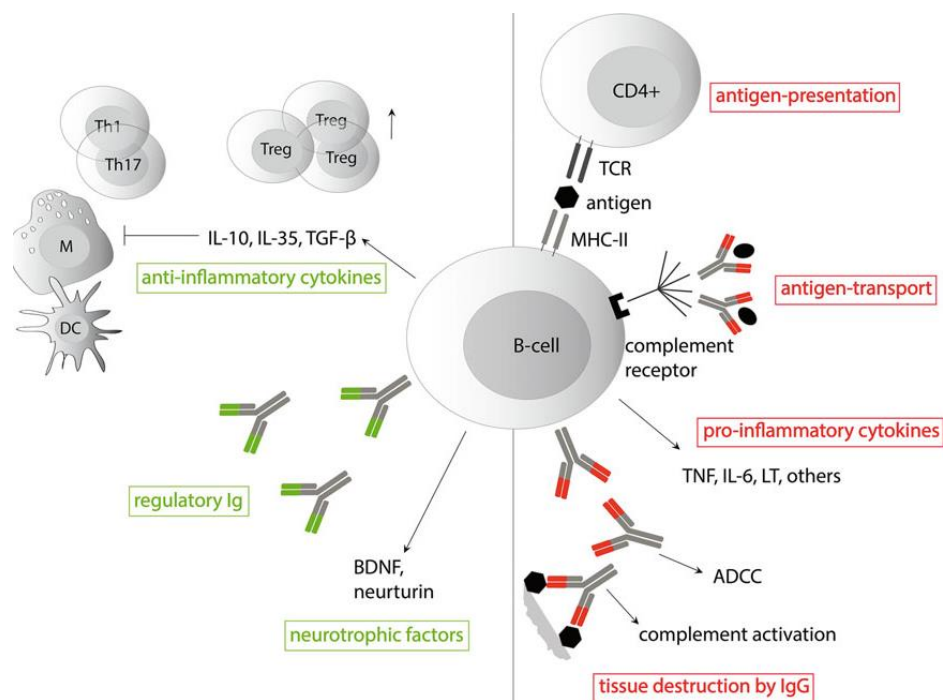


Figure 2: Inflammatory and regulatory functions of B cells. B cells exert various pro-inflammatory and immunoregulatory functions: They produce antibodies that can activate complement and ADCC. They are involved in the production and secretion of pro-inflammatory cytokines, antigen-presentation and follicular antigen-transport. On the other hand, they also produce anti-inflammatory cytokines and neurotrophic factors, as well as producing antibodies with potential immunoregulatory functions. Figure taken from (Hoffmann and Meinel 2014)

1.2 Therapeutic interventions targeting B cells and antibodies

Due to the pathogenic role of B cells and autoantibodies in CNS inflammation, there has been a strong development of new therapeutic approaches to directly and specifically target them.

Plasma exchange and immunoadsorption (IA) are used to remove circulating autoantibodies. These therapies are indicated for acute steroid-resistant relapses in MS and NMO patients (Heigl et al. 2013; Krumbholz and Meinel 2014).

B cell depletion can be accomplished using type I anti-CD20 monoclonal antibodies (mAb) and they have shown varying degrees of efficacy. Three of them, rituximab, ocrelizumab, and ofatumumab are currently in clinical use for MS. Rituximab, a chimeric mAb, depletes CD20⁺ B cells and reduces inflammatory brain lesions and clinical relapse in RRMS (Hauser et al. 2008) and some NMO patients also can benefit from it, since it reduces the levels of AQP4- specific antibodies (Pellkofer et al. 2011) (Jarius et al. 2016). Ocrelizumab is approved for RRMS and PPMS and differs from rituximab in that it has a humanized antibody backbone (Kappos et al. 2011; Montalban et al. 2017). Ofatumumab, a fully human monoclonal antibody, is used in RRMS where it has shown to reduce brain lesion in patients (Sorensen et al. 2014). A new class of type II anti-CD20 antibodies, obinutuzumab, a humanized IgG1, is under development (Niederfellner et al. 2011).

Anti-CD20 mAbs efficiently deplete mature naïve and memory B cells, inhibit the development of short-lived plasma cells, but spare long-lived plasma cells. Contrary to CD20, CD19 is expressed from early B cell development to the last differentiation stage including plasma cells. Inebilizumab (MEDI-551) is a human IgG1 anti-CD19 mAb that was developed for the treatment of relapsing MS and has shown the capability to completely delete B cells in a phase I trial (Agius et al. 2019).

2. Myelin Oligodendrocyte Glycoprotein (MOG)

MOG consists of 218 amino acids and belongs to the immunoglobulin superfamily (Pham-Dinh et al. 1993). MOG is a minor component of CNS myelin (less than 0.05%) and is located in the outermost surface of the myelin (Brunner et al. 1989). The exact function of MOG is still unknown, but its structure and localization suggest a role as an adhesion molecule (Clements et al. 2003) and in accordance, MOG expresses the L2/HNK1 epitope, which is a marker for cell adhesion (Burger et al. 1993). MOG is able to bind the complement component C1q and might be able to regulate the classical complement pathway (Johns and Bernard 1997). In addition, MOG extracellular immunoglobulin domain can bind to nerve growth factor (NGF) and its presence seems to help the rubella virus to entry the cells (Reindl and Waters 2019) A MOG knockout mouse, however, did not show any obvious phenotype (Delarasse et al. 2003).

Among many candidate antigens were proposed as antibody targets in MS and related disorders, MOG is by far the one that has received more attention. This is due to the fact that it is localized in the outermost surface of the myelin sheath and that makes it accessible for the pathogenic autoantibodies (Mayer and Meinl 2012; Reindl and Waters

2019). Further studies in animal models demonstrated that MOG is indeed a target for demyelinating antibodies (see part 4).

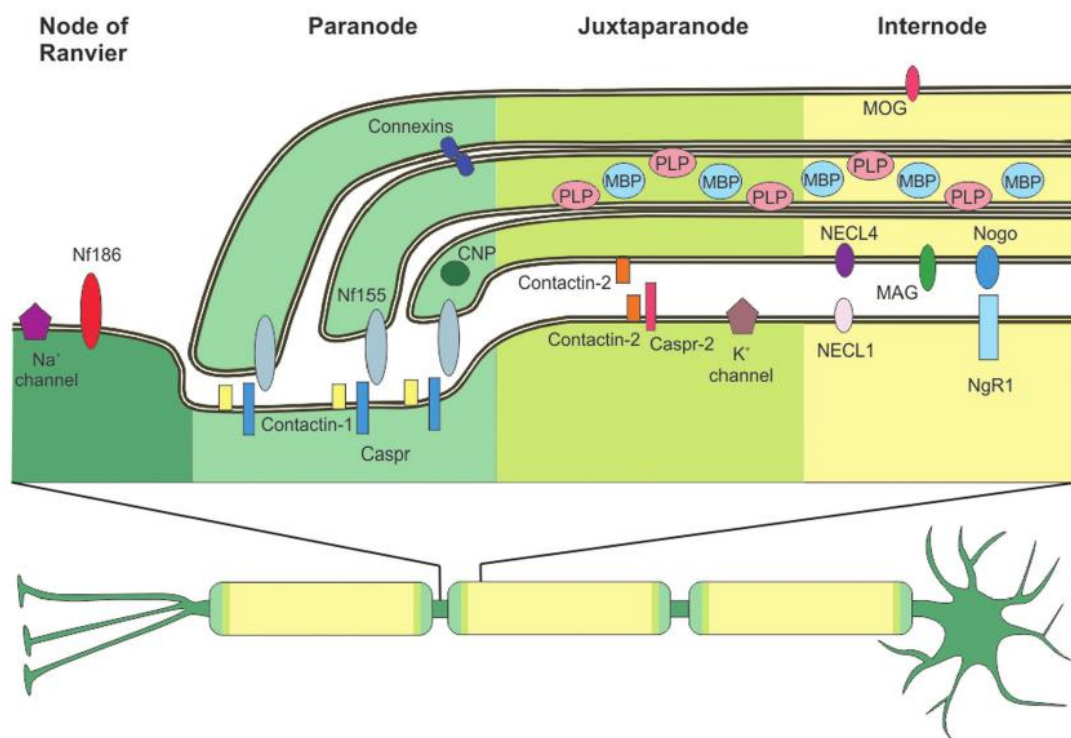


Figure 3: Distribution of CNS myelin protein: Common myelin proteins are found at the internode, the major myelin proteins are: Proteolipid protein (PLP) and Myelin basic protein (MBP). MOG is a minor component of the myelin and is located on the outermost surface of the myelin sheath. Figure taken from (Mayer and Mehl 2012).

3. N-glycosylation and its role in antibody binding

MOG has a single N-glycosylation site in Asn31 (N31) (Gardinier and Matthieu 1993). A second potential N-glycosylation site, Asn52, was found in mouse brain using tandem mass spectrometry, but it lacks the N-glycosylation consensus sequence N-IP-[SIT] and therefore it was not considered a high-confidence glycosylation site (Zielinska et al. 2010).

Some studies showed that using a MOG mutant, where the asparagine is substituted with aspartic acid, N31D mutant (O'Connor et al. 2007; Mayer et al. 2013) completely abolished MOG glycosylation. This aglycosylated MOG mutant is recognized at least as good as wild-type MOG (hMOG) and some patients (7%) recognized the N31D better than hMOG (Mayer et al. 2013; Spadaro et al. 2015). The higher recognition of N31D by the patients' autoantibodies might be due to better accessibility to MOG when it's lacking the polycarbohydrate chain at its upper, very exposed edge of its extracellular domain.

Previous studies have already highlighted the importance of glycosylation in antigen-antibody recognition. Deglycosylation of the HIV envelope glycoprotein gp120 leads to increase recognition by neutralizing antibodies (Koch et al. 2003) and changes in the glycosylation pattern of HIV envelope are involved in the escape of HIV mechanism from neutralizing antibodies (Wei et al. 2003). Moreover, a subgroup of patients with aggressive chronic inflammatory demyelinating polyradiculoneuropathy have autoantibodies against contactin and in some the immunoreactivity is dependent on N-glycans. Surprisingly, in one patient autoantibodies were selectively directed against contactin containing mannose-rich N-glycans (Labasque et al. 2014)

4. MOG antibodies

The first antibody responses against MOG were found on the sera of guinea pigs with chronic relapsing EAE induced by inoculation with homologous spinal cord in adjuvant. The serum of these guinea pigs was injected on the subarachnoid space of wild-type rats and was able to induce in vivo demyelination and anti-MOG titers correlated with this pathogenic demyelination (Linnington and Lassmann 1987). After that, evidences of the involvement in the pathogenesis of anti-MOG antibodies were found in Lewis rats (Adelmann et al. 1995), mice (Schluesener et al. 1987; Bourquin et al. 2003) and primates (Genain et al. 1995; Hart et al. 2004). It was observed in these animal models that, upon active immunization, MOG antibodies trigger an antibody-mediated demyelination.

EAE can be induced either by active immunization with MBP or with adoptive transfer of T cells, e.g. specific for MBP. In the absence of anti-MOG antibodies, EAE is characterized by inflammation, without any sign of demyelination. MOG antibodies induce demyelination in a complement dependent manner (Piddlesden et al. 1993) and require the breakdown of the blood-brain barrier to enhance pathology (Litzenburger et al. 1998). More recently, two studies showed that MOG antibodies can also enhance inflammation by increasing the antigen presentation to MOG-specific T cells in the CNS, helping them to be reactivated in the immune deprived CNS tissue (Flach et al. 2016; Kinzel et al. 2016).

4.1. MOG antibodies in patients and epitope mapping

The finding in EAE models clearly pointed out that MOG was a target candidate for human autoantibodies in CNS demyelinating diseases. It is well known, that only antibodies against conformational epitopes of MOG are associated with pathogenic demyelination (Mayer and Meinl 2012). Many studies have shown that anti-MOG

antibodies are found in 20-40% of children with ADEM, chronic relapsing inflammatory optic neuropathy, or paediatric MS (O'Connor et al. 2007; Mayer and Meinl 2012; Reindl and Waters 2019). In adult patients, antibodies to MOG have been detected in patients with AQP4-negative NMO spectrum disorder. Also, in special cases of MOG-antibody associated encephalomyelitis, in bilateral recurrent ON, and rarely in anti-NMDA-receptor encephalitis and in adults with MS (Reindl et al. 2013; Hohlfeld et al. 2016).

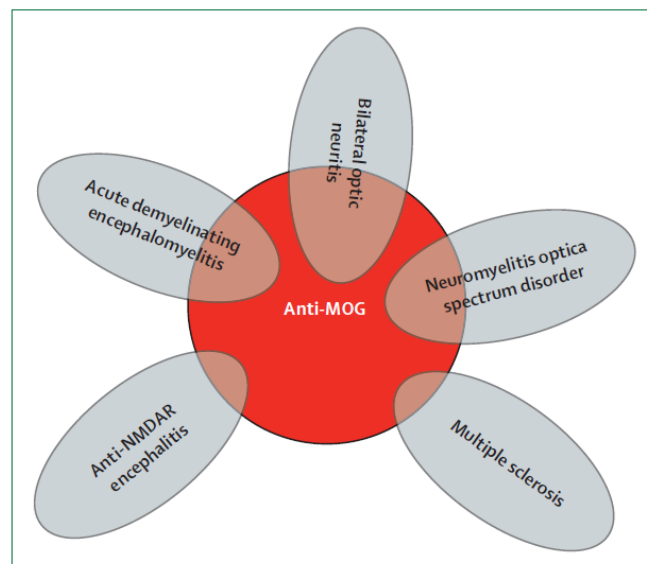


Figure 4: Overlapping features of MOG-antibody associated CNS disorders. Frequencies of antibodies against MOG found in patients with these diseases are indicated by the extent of overlap in the diagram. Figure taken from (Hohlfeld et al. 2016)

It is currently discussed whether MOG-abs constitute a separate disease entity (Weber et al. 2018)

A previous study in the lab, used a panel of MOG mutants to get an insight into the epitope determination on native human MOG in different paediatric patient groups. They reported that anti-MOG antibodies predominantly recognise epitopes that connect the β strands of the extracellular MOG domain. The most frequently recognized epitope was P42, which is only present in human MOG, but not rodent MOG. In addition, 20% of the patients had antibodies against the His103:Ser104 epitope, which is the main target of the mAb 8-18C5 used in animal studies. Longitudinal analysis showed that the individual epitope pattern remained constant, with no evidence of epitope spreading (Mayer et al. 2013)

5. Possible pathogenic mechanisms of MOG antibodies in humans

Most anti-MOG antibodies are IgG1 isotype and can bind and activate the complement pathway, as well as bind to the Fc receptors (McLaughlin et al. 2009). Also, a posterior study showed that at high titers, antibodies to MOG can activate the complement cascade, leading to the formation of the terminal complement complex (TCC) and to the internalization of these antibodies (Mader et al. 2011). Moreover, purified anti-MOG antibodies from children with clinically isolated syndrome (CIS) or ADEM have a natural killer mediated cytotoxic effect on MOG-expressing cells *in vitro* and antibody-dependent cell-mediated cytotoxicity (ADCC) correlated with antibody titers (Brilot et al. 2009).

The involvement of human MOG-specific antibodies in the pathogenesis is also supported by *in vivo* studies. Transfer of sera from anti-MOG positive MS patients to EAE rats showed an enhancement of demyelination and complement deposition (Zhou et al. 2006). A different study, demonstrated that MOG-IgG from NMO patients causes myelin changes and alters the expression of axonal proteins when injected in mice brains. These effects were reversible within two weeks and were largely independent of the complement pathway (Saadoun et al. 2014).

In addition, a previous study from the lab affinity-purified anti-MOG antibodies from patients' sera and co-transfected them with MOG or MBP-specific T cells in Lewis rats. Anti-MOG antibodies together with T cells were able to induce EAE pathology in rats. Together with MBP-specific T cells, anti-MOG antibodies were able to breach the BBB and induce demyelination and C9 neo activation, which resembles the MS II pathology. On the other hand, when transfected with MOG-specific T cells, anti-MOG antibodies enhanced T cell infiltration and directed macrophages to the subpial parenchyma (Spadaro et al. 2018).

5.1 Complement activation and Fc γ receptor activation as effector mechanisms of antibodies

Antibodies are key players in both, innate and adaptive immunity, and when produced in response to a foreign antigen, they can mediate host protection. Through their antigen-binding Fab domains, antibodies recognize their specific target antigen and the Fc domain is the responsible for mediating the diverse effector mechanisms triggered by this Fab-antigen interaction. Effector functions arise from the binding of the Fc domain to Fc- γ receptors (Fc γ R) and also the recruitment of the complement component C1q.

Fc γ receptors Fc γ R

Fc γ receptors (Fc γ R) are expressed in diverse leukocytes cell types and when they interact with IgG the result is a variety of effector functions, including endocytosis of immune complexes, antibody-dependent cell-mediated phagocytosis (ADCP), ADCC, and initiation of anti-inflammatory pathways that actively suppress immunity (Nimmerjahn and Ravetch 2008). In figure 5 the different human Fc γ R are shown with their function, affinity for IgG and their expression on different cell types.

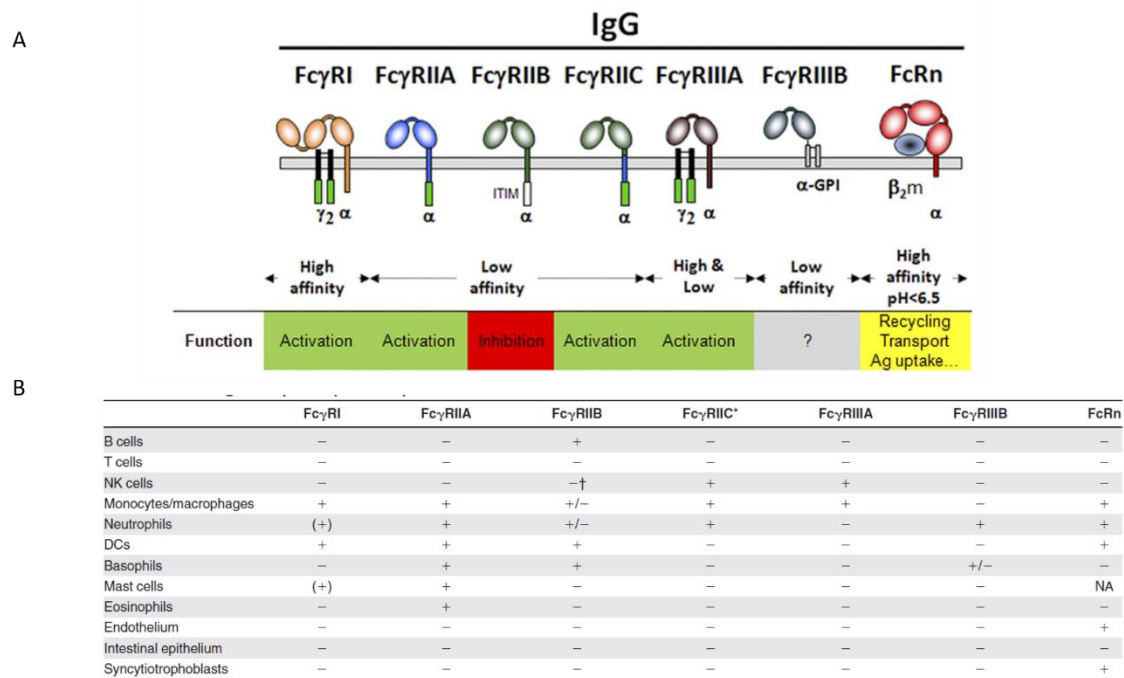


Figure 5: Human IgG receptors. (A) Schematic representation of human IgG receptors at the cell membrane (grey bar) and their association to the Fc γ R-chain dimer (black). Green boxes represent ITAMs; and the white box, the ITIM. (B) Human IgG receptor expression pattern. +, indicates expression; (+), inducible expression; +/-, very low percentages or rare subsets express the receptor; -, no expression; and NA, not analysed. † detectable and functional expression in nonconventional Fc γ R2c-Stop persons. Figure taken from (Bruhns 2018)

There are evidences that both, support and contradict, for a role of Fc γ R in MS and EAE. In favour, in active MS lesions reactive microglia are strongly stained for Fc γ RI, Fc γ RII and Fc γ RIII (Ulvestad et al. 1994). Also, several studies actively induced EAE with MOG in C57Bl/6 mice knockout for Fc γ R (lacking Fc γ RI, Fc γ RIII and Fc ϵ RI) and in DAB/1 mice knockout for Fc γ R (lacking Fc γ RI, Fc γ RIII and Fc ϵ RI) and mice lacking only the Fc γ RII (Lock et al. 2002; Abdul-Majid et al. 2002). These studies showed that Fc γ R deficient mice develop an attenuated EAE and that Fc γ RII deficient mice exhibited a more severe EAE compared to WT mice.. In the same line, in a more recent study they used mice transgenically expressing human Fc γ R and showed that Fc γ R interactions, especially

those involving FcγRIIA, are necessary and sufficient for MOG induced EAE exacerbation (Khare et al. 2018). Furthermore, functional expression of FcγR on systemic accessory cells, but not CNS-resident cells is vital for the development of CNS inflammation, independent of antigen-presenting cell function or Ab involvement (Urich et al. 2006). These studies highlighted the importance of FcγRs during the development of inflammation in the CNS. On the other hand, EAE was induced by injecting MOG 35-55 peptide in FcγR and C1q knockout mice, and they established that the demyelinating capacity of anti-MOG antibodies *in vivo* relies entirely on complement activation and is FcR-independent (Urich et al. 2006).

Previous studies have provided a comprehensive mapping of the binding sites on human and murine IgG for the different FcγR and determined that the lower hinge region, composed of residues Leu²³⁴-Pro²³⁸, Ala³²⁷ and Pro³²⁹, are primarily the responsible for the IgG-FcγR interaction. Further studies proposed additional segments for each individual FcγR, e.g. for human FcγRI Gly³¹⁶-Lys³³⁸ and for FcγRIII Lys²⁷⁴-Arg³⁰¹ and Tyr⁴⁰⁷-Arg⁴¹⁶. Amino acid substitutions in these residues can modify IgG- FcγR binding. For example. L235A or P329A mutations diminish IgG binding to all FcγR, while other mutation can improve IgG recognition to some FcγR, T256A or K290A improve IgG binding to FcγRII and FcγRIIIA (Shields et al. 2001).

Complement

Complement is a key component of the innate immunity that serves as a first line of defence against foreign and altered host cells. It is composed of plasma proteins which are mostly produced by the liver or membrane proteins expressed on the cell surface (Merle et al. 2015). Activation of the classical complement cascade leads to: direct cell lysis through complement-dependent cytotoxicity (CDC) and to the deposition of opsonins which trigger complement-dependent cell-mediated cytotoxicity (CDCC) and complement-dependent cell-mediated phagocytosis (CDCP). In addition, activation of the classical pathway stimulates B and T cell adaptive responses (Hess and Kemper 2016).

There are many evidences that demonstrate a role of the complement system in MS pathogenesis. Among many others, deposition of complement components and activation products have been found in the white matter plaques in MS brain tissue. Moreover, a complement dysregulation is also found in MS gray matter lesions, supporting that complement activation and dysregulation occur in all MS cases. (Tatomir et al. 2017)

A recent paper from our group, showed that patient-derived MOG-specific antibodies enhanced immune cell infiltration and induce demyelination with complement activation in a EAE rat model (Spadaro et al. 2018). Furthermore, anti-MOG antibodies could activate the complement cascade in vitro, resulting in the formation of the terminal complement complex (TCC) (Mader et al. 2011). On the other hand, MOG-specific human IgG1 antibodies that lack the ability to bind mouse complement, do not affect the ability of these antibodies to increase EAE disease activity (Khare et al. 2018)

The region comprising the amino acids 318-337 is of the segments of the CH2 domain which binds to C1q. Specifically, C1q appears to interact with the charged side chains of residues Glu³¹⁸, Lys³²⁰ and Lys³²². Mutations in these positions lower the IgG affinity for C1q binding (Duncan and Winter 1988). Further studies also showed that site directed mutagenesis in the Pro³³¹ of IgG also reduces C1q recognition (Tao, Smith, and Morrison 1993). Also, there are mutations that can improve complement binding, i.e amino acids substitutions K326W and E333S, produced a 9-fold increase in CDC (Ratelade et al. 2013).

5.2 Role of Fc glycosylation

Differences in the glycosylation of the Fc fragment modulates the effector function of IgG. An N-glycan is covalently attached to the side chain nitrogen atom of the highly conserved Asn²⁹⁷ of both heavy chains. The majority of these glycans are complex-type biantennary structures, however, a high degree of heterogeneity exists due to the presence of different monosaccharides. Differences in Fc glycosylation result in altered binding affinity for FcγRs and complement, which ultimately influences the effector mechanisms. For example, the presence of a core fucose (fucosylation) or the addition of N-acetylneuraminic acid (Neu5Ac) (sialylation) may have a decreased affinity for FcγRIIIa leading to an anti-inflammatory effect (Quast and Lünemann 2014; Russell et al. 2018).

It is widely accepted that reducing the level of glycosylation in the Asn²⁹⁷ by EndoS treatment (an enzyme that cleaves the sugar moiety after the first GlcNac) or the absence of glycosylation due to site directed mutagenesis, reduces or abolishes the capability of IgG to bind to FcγRs and complement (Arnold et al. 2007). In addition, a more recent study showed that mouse IgG2c and human IgG1 and IgG3 subclasses maintain their in vivo activity when the glycan is composed of a mono- or disaccharide sugar residue via binding to FcγRs, but are unable to activate the complement pathway (Kao et al. 2015)

Objectives

The main aims of this study were:

- Asses the role of the MOG glycosylation site in autoantibody recognition and further identify the glycoforms on HEK EBNA derived MOG and in human myelin derived MOG using Mass spectrometry.
- Determine the effector functions of the mAb r8-18C5. Generate a panel of muatated variants of the anti-MOGI mAb r8-18C5 with mutations on their Fc part and test them for their binding to complement and FcγR, using ELISA and luciferase reporter assays.

Materials and Methods

6. Materials

Patient material

This study included sera of 27 patients with different inflammatory CNS diseases and healthy controls. Sera were provided by the medical team of the Institute of clinical Neuroimmunology of the Klinikum Großhadern (Munich, Germany) and Hacettepe University (Turkey). Original samples were stored at -80°C while working aliquots were stored at -20°C.

Table 1: Details of the anti-MOG positive patients.

Patient ID ¹	Diagnosis ²	Treatment at the point of blood drawn	Sex	Age
1	LETM	None	F	22
2	MS	Teriflunomide	F	60
3	MS/NMOSD	Steroids + Teriflunomide	F	47
4	ADEM	None	F	35
5	CIS	None	F	47
6	Relapsing ON	None	F	52
7	MS	Natalizumab	M	39
8	NMOSD	Cyclophosphamide	M	32
9	ON	None	F	60
10	RON	Rituximab	F	34
11	RON	Rituximab	M	43
12	ON	Azathioprine	M	37
13	NMOSD	Azathioprine	M	35
14	BON	Azathioprine	F	35
15	Relapsing encephalomyelitis	Steroids + Plasmapheresis	M	42
16	Relapsing ON	None	F	48
17	Relapsing encephalomyelitis	Azathioprine	F	72
18	Relapsing encephalomyelitis	Steroids	M	35
19	MS	Glatiramer acetate	F	60
20	NMOSD	Azathioprine	M	45
21	NMOSD	None	M	42
22	Relapsing ON	Azathioprine	M	51
23	NMOSD	Glatiramer acetate	F	38
24	Monophasic encephalitis	None	F	36
25	Relapsing ON	None	F	35
26	Relapsing ON	None	M	57
27	NMSOD	Steroids	M	33

¹Some patients have been previously described in more detail: Patient 17 in (Spadaro et al. 2015) patients 7 and 19 in (Spadaro et al. 2016) and patients 15,16,22,23,25,26 and

27 in (Spadaro et al. 2018). ²We give the original diagnosis; It is currently discussed whether patients with MOG-Abs constitute a separate disease entity (Zamvil and Slavin 2015; Jurynczyk et al. 2017; Di Pauli and Berger 2018; Jarius et al. 2018). LETM, longitudinal extensive transverse myelitis; NMOSD, neuromyelitis optica spectrum disorder; ADEM, acute disseminated encephalomyelitis; CIS, clinically isolated syndrome; ON, optic neuritis; RON, recurrent optic neuritis; BON, bilateral optic neuritis

7. Methods

7.1 Mutagenesis

Using the “QuickChange Site-Directed Mutagenesis” kit (Stratagene, Santa Clara, CA, USA), point mutations were introduced into hMOG, using the vector MOG-EGFP-N1 as a template and the primers shown in Table 2 and the corresponding reverse complement primers.

Table 2: Primers used for hMOG aglycosylated mutants

Mutation	Sequence forward primer
N31D	5'-CAT ATC TCC TGG GAA GGA CGC TAC AGG CAT GGA GG-3'
N31A	5'-CAT ATC TCC TGG GAA GGC AGC TAC AGG CAT GGA GG-3'

The same protocol was used to generate the different 8-18C5 variants from the wild-type vector 8-18C5 in the pTT5 vector (provided by Dr. Dieter Jenne)(Perera et al. 2012). In this case the primers shown in Table 3 were used for the mutagenesis and the aglycosylated mutants were always obtained using the T319L primers on the previously cloned variant.

Table 3: Primers used for the 818C5 variants

8-18C5 variant	Mutation(s)	Sequence forward primer
Aglycosylated 8-18C5	T319L	5'-CAG TAC AAC AGC TTA TAC CGG GTG-3'
G801	K340E	5'-GGC AAA GAG TAC GAG TGC AAG TGT C-3'
	Q406R	5'-CAA CGG CAG ACC CGA GAA CAA C-3'
G802	L255K	5'-GAA CTG AAG GGA GGC CCT AG-3'

	G246M	5'-GAA CTG AAG ATG GGC CCT AG-3'
	G247R	5'-CGA ACT GAA GAT GAG ACC TAG CG-3'
	L351Q	5'-GGT GTA CAC ACA ACC CCC TAG C-3'
G803	A350S	5'-GCC TTC ACC CAT CGA GAA AAC-3'
	P351S	5'-GCC TTC ATC CAT CGA GAA AAC-3'
K342A	K342A	5'-GAG TAC AAG TGC GCA GTG TCC-3'
G804	K346W	5'-GTC CAA CTG GGC CCT GCC-3'
	E353S	5'-CCC CAT CTC AAA AAC CAT CAG C-3'

Table 4: Reagents for the PCR reaction

Reagent	Stock concentration of reagent	Final concentration
DNA template	-	50 ng
dNTPs	10mM	200 μ M
5x Phusion GC Buffer	5x	1x
Forward primer	10 μ M	0.5 μ M
Reverse primer	10 μ M	0.5 μ M
Nuclease-free water	-	To 50 μ l
DMSO	-	3%
Phusion DNA polymerase	-	2.0 units/50 μ l PCR

Table 5: PCR program

Stage	Temperature	Time	
Denaturation	98°C	30 seconds	
Denaturation	98°C	10 seconds	35 repeats
Annealing	68-72 °C (depending on the primer)	30 seconds	
Extension	72°C	3 minutes	
Extension	72°C	10 minutes	
Cooling	4°C		

7.2 Transformation of competent bacterial cells by heat shock

Plasmid amplification was done using competent NEB 5- α Competent *E.coli* (High efficiency) (New England Biolabs, Ipswich, MA, USA). For the transformation of NEB 5- α Competent *E.Coli*, 100 ng of plasmid DNA was used to transform 50 μ l of thawed bacterial cells. Cells were incubated for 30 minutes on ice and then heat-shocked for 90 seconds at 42°C, followed by a 5 minutes incubation on ice. Then, 900 μ l of SOC medium (Invitrogen, Karlsruhe, Germany) were added to the cells and they were place on a shaker at 180 rpm for 1 hour at 37°C. Afterwards, cells were centrifuge at 4000 rpm for 5 minutes and the supernatant was discarded, all except 50-100 μ l. Cells were resuspended and plated on LB-Amp agar or LB-Kan and incubated overnight at 37 °C. LB medium (for 1 L in water) consisted of: 10 g Bacto-tryptone (BD Biosciences, Heidelberg, Germany), 5 g yeast extract (BD Biosciences), and 10 g NaCl (Sigma-Aldrich, Germany); it was brought to pH 7.5 using NaOH and sterilized by autoclaving. For LB-agar, 15 g of agar were dissolved in 1L of LB and sterilized by autoclaving. For LB-Amp agar, ampicillin (Sigma-Aldrich, Darmstadt, Germany) was added to a final concentration of 100 μ g/mL, while for LB-Kan agar, kanamycin (Sigma-Aldrich) was added to a final concentration of 50 μ g/ml. 20 mL of LB agar was poured onto 10 cm culture plate (Greiner, Frickenhausen, Germany) for casting and the plates were stored at 4 °C until use.

7.3 Plasmid preparation

Plasmids DNA was purified from the overnight cultures using the Qiaspin Miniprep kit (Qiagen, Hilden, Germany) and following the protocol provided by the manufacturer. The purified DNA was sent for sequencing to the LMU Biocenter (Martinsried, Germany).

7.4 Cell culture of HeLa cells

HeLa cells were cultivated in T75 cell culture flasks (BD Biosciences) at 37 °C and 10% CO₂. Cells were passaged every 48 hours at a 1:10 ratio. In detail, cell culture medium was removed, cells were washed with 10 ml PBS (Invitrogen) and 2 ml Trypsin-EDTA (Invitrogen) were added. Cells were incubated for 5 minutes at 37 °C and trypsinization was neutralized by adding 8 ml of culture medium.

<u>HeLa culture medium</u>	<u>Dulbecco's modified Eagle Medium (DMEM) (Invitrogen)</u> 10 % fetal calf serum (FCS) (Gibco, Karlsruhe, Germany) 1 % Penicillin/Streptomycin (Gibco)
----------------------------	---

7.5 Cell culture of HEK 293 EBNA 1 cells

HEK 293 EBNA 1 cells (provided by Dr. Dieter Jenne) (Perera et al. 2012) were cultured in suspension in an incubator (Multitron Pro) with humidified atmosphere at 37 °C, 8 % CO₂ and 110 rpm. Cells were passaged every 48-60 hours to a density of 200.000 cells/ml.

<u>HEK 293 EBNA 1 culture medium</u>	<u>Freestyle 293 Expression medium (Gibco)</u> 1 % Pluronic F-68 10 % (Gibco) 25 µg/ml Geneticin G418 (Gibco)
--------------------------------------	---

7.6 Cell culture of TE cells

TE cells (Pröbstel et al. 2011) were cultivated in T75 cell culture flasks (BD Biosciences) at 37 °C and 5% CO₂. Cells were passaged every 48 hours at a 1:10 ratio. Briefly, cell culture medium was removed, cells were washed with 10 ml PBS (Invitrogen) and 2 ml Trypsin-EDTA (Invitrogen) were added. Cells were incubated for 5 minutes at 37 °C and trypsinization was neutralized by adding 8 ml of culture medium.

<u>TE culture medium</u>	<u>Complete Roswell Park Memorial Institute (RPMI)(Sigma)</u> 10 % fetal calf serum (FCS) (Gibco) 1 % Penicillin/Streptomycin (Gibco) 1% Sodium pyruvate (Gibco) 1 % Non-essential Amino Acids (Sigma) 10 mM L-glutamine (200mM, Gibco)
Selection antibiotic	2mg/ml of Geneticin (G418) (Invitrogen)

7.7 Transfection of HeLa cells with jetPRIME

HeLa cells were seeded in a 100 mm culture dish (BD Bioscience) at a density of 0.2×10^6 cells/ml. After 24 h cells were transiently transfected with jetPRIME (Polyplus, Illkirch, France) according to the instruction of the manufacturer. In detail, 15 µg of DNA were diluted in 500 µl of jetPRIME buffer and vortex for 10 seconds. Then, 30 µl of jetPRIME was added and the mix was again vortex for 10 seconds. After 10 minutes incubation at room temperature, the mixture was added to the cells for 24 hours.

7.8 Transfection of HEK 293 EBNA 1 cells

The heavy and light chains of the 8-18C5 antibody and its variants were expressed in serum free condition in suspension HEK 293 EBNA 1 cells. Cells were adjusted for transfection to a density of 1×10^6 cells/ml. Polyethylenimine (PEI) transfection reagent (Polypro Transfection) (Polyplus) and DNA were added separately to Optipro serum free transfection reagent (Invitrogen), mixed and incubated for 30 minutes at RT. 1 µg DNA and 2 µg PEI were used for 1 ml of cell suspension. Optipro was used in a volume corresponding to 1/10 of the cell suspension volume. The transfection mixture was added dropwise to the cell suspension. After 24 h incubation, Bacto TC Lactalbumin Hydrolysate (BD Biosciences) was added to a final concentration of 0.5 %.

7.9 Purification of recombinant protein by immobilized affinity chromatography (IMAC)

His Trap HP columns (GE Healthcare, Penzberg, Germany) were used to purify recombinant human MOG and the 818C5 antibody and its mutants from the supernatant of HEK 293 EBNA 1 cells. The antibodies carry a C-terminal 6x His-tag which allows the binding to the nickel on the column. The culture supernatants were centrifuged at 1000 rpm for 5 minutes at 4 °C, transferred to a new centrifuge tube and centrifuged again at 3500 rpm for 20 minutes at 4 °C. As a next step, culture supernatants were filtered through a 0.22 µm filter (Merck Millipore, Darmstadt, Germany). Supernatants were dialyzed overnight at 4°C against binding buffer (100 mM Na_2HPO_4 , 500 mM NaCl, 10 mM imidazole, pH 7.4). For purification, the column was equilibrated with 10 column volumes binding buffer, then the sample was applied. Column was washed with 10 column volumes binding buffer and then bounded protein was eluted by performing a linear imidazole gradient from 10 mM to 1 M imidazole. Wash and elution fraction were analyzed by SDS-Page, the fractions containing the purified protein were pooled and dialyzed against PBS overnight at 4 °C.

7.10 Deglycosylation by PNGase F

In order to analyze the glycosylation of the different MOG-EGFP constructs, HeLa cells were transiently transfected with MOG-EGFP constructs, as described above. The cells from a 10 mm dish were suspended in 1 mL PBS then pelleted at 3000 rpm for 5 minutes in a bench top centrifuge. The cells were then lysed at 4°C for 1h in 1 mL RIPA buffer (150 mM NaCl, 1% NP-40, 0.5% sodium deoxycholate, 50 mM Tris pH8, 0.1% SDS) containing complete protease inhibitor cocktail (Roche Applied Science, Penzberg, Germany). The lysate was then pelleted at 14000 rpm for 15 minutes and the supernatant was analyzed.

For deglycosylation, the supernatant was digested with PNGaseF (New England Biolabs) in Glycoprotein Denaturing Buffer (New England Biolabs), Glycobuffer 2 (New England Biolabs) and 1% NP40 (New England Biolabs) at 37°C overnight. PNGase digestion was also used in the different 8-18C5 variants and the same protocol was used.

7.11 Determination of protein concentration

Protein concentration was measured by using the Bicinchoninic acid (BCA) protein assay kit (Pierce, Rockford, IL, USA) according to the instructions of the manufacturer.

7.12 Sodium Dodecyl Sulfate polyacrylamide gel electrophoresis (SDS PAGE)

Gel electrophoresis was performed by using 4-12 % Bis Tris gels (Invitrogen) and an Xcell Mini Cell electrophoresis chamber (Invitrogen) filled with NuPAGE MOPS SDS Running buffer (Invitrogen). Samples were prepared by adding to 1-2 µg of protein NuPAGE LDS sample buffer (Invitrogen) and, if electrophoresis was performed under reducing conditions, NuPAGE sample reducing agent (Invitrogen). The samples were then incubated at 95 °C for 5 minutes and then loaded on the gel. Electrophoresis was carried out at 160 V for 90 minutes.

10x NuPAGE MOPS SDS Running buffer

250 mM Tris

1.92 M Glycine

1 %(g/V) SDS

7.13 Protein detection by Coomassie blue staining

After gel electrophoresis, gels were incubated on a shaker for 15 minutes with Coomassie blue staining solution (0.1 % Coomassie brilliant-blue R-250, 40 % methanol, 10 % acetic acid) followed by incubation for 1 hour with destain solution (50 %methanol, 7 % acetic acid). Destain solution was changed from time to time. Gel was stored overnight in a 7 % acetic acid solution at RT.

7.14 Western blot

The proteins were electro-blotted onto a nitrocellulose membrane at 60mA for 90 minutes. The membrane was blocked on PBS containing 5% milk for 1h at room temperature. The membrane was incubated with the primary antibody diluted in 5% milk overnight at 4°C. Next day, the membrane was washed three times and incubated with the secondary antibody diluted in 5% milk for 1 hour at room temperature and then washed three times. The blots were developed using the Immobilion Western kit used (Millipore, Massachusetts, USA) and the Odyssey Fc Imaging system (LI-COR, Bad Homburg, Germany).

Table 6: Antibodies and their dilutions used in the Western blots

Antibody	Type	Dilution	Company
8-18C5	primary	1/500	-
Anti-MBP	primary	1/3000	Merck, Darmstadt, Germany
Anti-GFP-HRP	secondary	1/5000	Genetex, California, USA
Anti-mouse-HRP	secondary	1/2500	Promega, Wisconsin, USA

7.15 Enzymatic biotinylation of hMOG

hMOG was biotinylated by using the BirA biotin ligase Kit (Avidity, Aurora, CO, USA) according to the instruction of the manufacturer. The final reaction mixture was incubated overnight at 30 °C. Free biotin was removed by using 3 K centrifugal filters (Merck Millipore) and the sample was suspended in PBS (Invitrogen). Biotinylated hMOG was used to perform the C1q binding affinity of 8-18C5 variants and also to assess their binding to hMOG.

7.16 Serum screening for MOG-Abs by FACS

Autoantibodies against conformationally intact MOG were detected by performing a cell-based flow cytometry assay. HeLa cells were transiently transfected with full length hMOG fused C-terminally to the EGFP N1 (CLONTECH Laboratories, Mountain View, CA, USA) vector or with EGFP alone (control cells). 24 hours after transfection, cells were plated in a 96 well FACS plate at a density of 50.000 cells/ well. Cells were pelleted by centrifuging them at a speed of 400 g for 5 minutes. Control and MOG-transfected cells were incubated with 100 μ l of a 1:50 dilution of each serum and incubated for 45 minutes at 4 °C. As a next step, cells were washed three times with 150 μ l PBS/ 1 % FCS. MOG-specific IgG was detected with 100 μ l of a 1:500 dilution of a biotin-SP-conjugated goat anti-human IgG (Jackson ImmunoResearch, West Grove, PA, USA). Cells were incubated for 30 minutes at 4 °C. After three washing steps, cells were incubated with 100 μ l of a 1:2000 dilution of Alexa Fluor® 647-conjugated Streptavidin (Jackson ImmunoResearch) and incubated in the dark for 30 minutes at 4 °C. After three washes, dead cells were stained with 100 μ l of propidium iodide (Sigma-Aldrich) diluted 1:2000 in PBS. FACS analysis was performed on a BD FACSVerse flow cytometer and data was analyzed with FlowJo (Tree Star Inc., Ashland, OR, USA). The human recombinant 8-18C5 was used as a positive control at a concentration of 0.5 μ g/ml. The same protocol was used for the determination of the 8-18C5 variants affinity to MOG, with an antibody concentration of 0.5 μ g/ml. Binding affinity was calculated as mean fluorescence intensity (MFI) (mutant) / MFI (EGFP only). The 8-18C5 variants were also tested for their affinity to MOG using an anti-Histidine-peroxidase (Merck) as a primary antibody and an anti-HRP Alexa Fluor® 647 (Jackson ImmunoResearch).

7.17 Binding of recombinant 8-18C5 variants to hMOG

Recombinant antibodies were also tested by ELISA to assess their affinity to hMOG. In detail, immobilized on a streptavidin coated 96 well plate (Nunc, Thermo Scientific, Karlsruhe, Germany) were coated with biotinylated hMOG for 2 hours at room temperature 100 μ l/well diluted in coating buffer (100 mM sodium carbonate, pH 9.5) to a final concentration of 1 μ g/ml. After washing three times, each well was incubated overnight at 4°C with the recombinant antibodies diluted in incubation buffer (0.5 % BSA in PBS). Antibodies were serially diluted from a concentration of 10 μ g/ml to 0.001 μ g/ml. Negative control antibody was used at the same concentrations. Next day, after three washes, each well was incubated with 100 μ l of a 1:5000 dilution of a horseradish peroxidase labeled goat anti-human IgG (Jackson Immuno Research) in the dark for 1 hour at RT on a shaker. After washing, 100 μ l of TMB (Sigma-Aldrich) were added and

the reaction was stopped after 7-8 minutes by using 50 μ l of 1 M sulfuric acid. Optical density was measured with a Victor2 plate reader (Perkin Elmer Life Sciences, Waltham, MA, USA) at 450 nm and 540 nm for plate background. The anti-MOG reactivity was calculated as follows: Δ OD (450 nm-540 nm).

7.18 C1q binding of recombinant 8-18C5 variants

Recombinant antibodies were also tested by ELISA to their ability to bind to C1q. The same protocol than in section x was used, with the following modifications. After the overnight antibody incubation and the washes, each well was incubated with 100 μ l of complement component C1q (Sigma-Aldrich) with a concentration of 10 μ g/ml for 2 hours at RT. After three washes, each well was incubated with 100 μ l of a 1:200 dilution of a HRP labeled anti-C1q (LsBio, Seattle, WA, USA) for 30 minutes at RT on a shaker. The detection was done as described above.

7.19 Purification of hMOG-EGFP from HeLa cells using His-tag dynabeads

His-Tag dynabeads (Invitrogen), previously bound with 8-18C5, were used to purify the hMOG-EGFP protein from transiently transfected HeLa cells. In order to purify hMOG-EGFP protein, HeLa cells were transiently transfected with hMOG-EGFP construct, as described above. The cells from a 10 mm dish were suspended in 1 mL PBS then pelleted at 3000 rpm for 5 minutes in a bench top centrifuge. The cells were then lysed at 4°C for 1h in 1 mL Pull-down buffer (3.25 mM sodium phosphate, 60 mM NaCl, 0.02% Tween, pH 7.4) with an addition of Tween until reaching a 0.5% and containing complete protease inhibitor cocktail (Roche Applied Science). The lysate was then pelleted at 14000 rpm for 15 minutes and the supernatant was run through the His-tag dynabeads. For the purification, 2 mg of dynabeads magnetic beads were placed in a 1.5 ml tube and incubated with 40 μ g of the 818C5 diluted in 700 μ l of binding/washing buffer (50 mM sodium phosphate, 300 mM NaCl, 0.02% Tween, pH 8). As mentioned above, the 818C5 contains a His-tag which allows the binding to the nickel on the column. After 10 minutes incubation on a roller at room temperature, the beads were washed 4 times with washing buffer. Then, the HeLa cells supernatant was diluted in pull-down buffer and incubated for 30 minutes on the roller at room temperature. After 4 washes, the His-tag dynabeads were incubated with His elution buffer (300 mM Imidazol, 50 mM sodium phosphate, 300 mM NaCl, 0.01% Tween) for 5 min on the roller and at room temperature. The elution fraction was stored at 4°C for further analysis.

7.20 Purification of myelin glycoproteins from bovine brain with Lentil-lectin sepharose 4B column

Approximately 50 grams of bovine brain was homogenized in 240 ml 0.32 M sucrose and the addition of complete protease inhibitor cocktail (Roche Applied Science). The homogenate was centrifuged at 500g for 10 minutes at 4°C. The next steps were all carried out by a SW32 Ti rotor in the ultracentrifuge at 4°C. The supernatant was further centrifuged at 9100 rpm for 33 minutes. The supernatant was discarded and the pellets were resuspended in 0.32 M sucrose and centrifuged again at 9100 rpm for 33 minutes. This step was repeated once more. Then, the pellets were resuspended in 16 ml 0.32 M sucrose, overlaid on 10 ml of 0.85 M sucrose and centrifuged at 12000 rpm for 43 min. The myelin fraction collected in the interphase was diluted with equal amounts of distilled water and centrifuged at 9100 rpm for 33 minutes. The pellets were resuspended with 200 ml of distilled water and homogenized for 30 minutes at 4°C on a rotary shaker and then they were centrifuged at 9100 for 33 minutes. The pellets were again homogenized as described above in 0.32 M sucrose overlaid in 0.85 M sucrose and centrifuged. Myelin proteins were separated in the interphase, diluted with distilled water and centrifuged as previously described. Finally, proteins were washed three times in distilled water and lysed overnight at 4°C in a rotary shaker with lysis buffer (3% Na-deoxycholat, 20 mM Tris, pH 8).

In order to prepare the myelin proteins for the lentil-lectin sepharose 4B column (GE Healthcare) they were dialyzed against binding buffer (0.5% Na-deoxycholat, 20 mM Tris, pH 8) overnight at 4°C. Next day, the column was equilibrated with 10 column volumes binding buffer and then the myelin proteins were run through the column. After 10 column volumes of washing buffer (20 mM Tris, pH 8) the myelin glycoproteins were eluted from the column with elution buffer (0.3 M methyl- α -D-mannopyranosid, 20 mM Tris, pH 7.4). The myelin glycoprotein fractions were kept at -80°C until further analysis.

7.21 ADCC activity of the 8-18C5 variants using murine Fc γ RIII effector cells

The 8-18C5 mutants were tested for their ability to activate mFc γ RIII using an ADCC reporter bioassay (Promega, Madison, WI, USA), the kit was used according to manufacturer's instructions. Briefly, in a 96-well plate, 75.000 cells/well of effector cells mFc γ RIII were incubated with 25.000 cells/well of TE MOG cells (target cells). Afterwards, 5 μ g/ml of the different 8-18C5 mutants were added in each well. The antibody-cells mixtures were incubated for 12 hours at 37°C.

Then, the 96-well plates were equilibrated to room temperature for 15 min and 75 μ l of Bio-Glo Reagent was added in each well. After 20 minutes incubation, luminescence was measured.

7.22 Preparation of ethyl esterified released N-glycans from recombinant MOG

An SDS-PAGE gel band corresponding to HEK cell derived MOG (15-20 μ g, migrating at ~21 kDa) was reduced, alkylated and subsequently treated with N-glycosidase F (PNGase F; Roche Diagnostics, Mannheim, Germany) to release the N-glycans, as described previously (36). Additionally, 5 μ g of HEK derived MOG was denatured and incubated overnight with PNGaseF in-solution at 37 °C (37, 38). Released N-glycans were subjected to the selective ethyl esterification of sialic acids, thereby introducing mass differences of +28.03 Da and -18.01 Da for α 2,6-linked N-acetylneuraminic and α 2,3 N-acetylneuraminic acid, respectively (37). Briefly, released glycans were incubated with the derivatization reagent (250 mM 1-ethyl-3-(3-(dimethylamino)propyl)carbodiimide and 250 mM 1-hydroxybenzotriazole in ethanol) and incubated for 60 min at 37°C. The derivatized glycans were enriched by cotton hydrophilic-interaction liquid chromatography (HILIC)-solid-phase extraction (SPE) as described before (39) and eluted in water.

7.23 MALDI-TOF(/TOF)-MS(/MS) analysis of released glycans

MALDI-TOF-MS analysis was performed on an UltrafleXtreme (Bruker Daltonics, Billerica, MA, USA) operated under flexControl 3.3 (Build 108; Bruker Daltonics). Two and 5 μ L of the enriched ethyl esterified glycans were spotted on a MALDI target (MTP AnchorChip 800/384 TF; Bruker Daltonics) together with 1 μ L of super-DHB (5 mg/mL in 50% ACN and 1 mM NaOH). The spots were dried by air at room temperature. For each spot, a mass spectrum was recorded in the range from m/z 1000 to 5000, combining 10000 shots in a random walk pattern at 1000 Hz and 200 shots per raster spot. Prior to the analysis of the samples, the instrument was calibrated using a peptide calibration standard (Bruker Daltonics). Tandem mass spectrometry (MALDI-TOF/TOF-MS/MS) was performed for the most abundant glycans using laser-induced dissociation, and compositions as well as structural features of N-glycans were assessed on the basis of the observed fragment ions.

Tandem mass spectrometry (MALDI-TOF/TOF-MS/MS) was also used to identify the glycans from myelin derived MOG.

Data processing

For automated relative quantification of the released glycans, the MALDI-TOF-MS files were converted to text files and analyzed using MassyTools (version 0.1.8.1.) (40) . Spectra were internally calibrated using glycan peaks of known composition with a S/N above nine, covering the m/z range of the glycans. Integration was performed on selected peaks from all glycans that were observed. For this, at least 95% of the theoretical isotopic pattern was included. Several quality parameters were used to assess the actual presence of a glycan i.e. the mass accuracy (between -10 and 10 ppm), the deviation from the theoretical isotopic pattern (below 25%) and the S/N (above three) of an integrated signal. Analytes were included for relative quantification when present in at least half of the technical replicates (excluding poor quality spectra), resulting in a list of 58 glycans. Finally, only glycans with an intensity covering at least 1% of the overall glycan abundance were selected, resulting in 28 glycans that were relatively quantified (as a fraction of the total glycan signal intensity).

7.22 and 7.23 were done by Dr. Paul Hensberger and Agnes L. Hipgrave Ederveen from the lab of Prof. Dr. Manfred Wuhrer, Leiden. They provided the text of these paragraphs for the thesis.

7.24 Statistics

We tested 27 anti-MOG positive patients with wild-type MOG and two aglycosylated variants of MOG, N31A and N31D. Each serum was tested with each MOG variant 4-5 times. A difference between two MOG variants was considered significant if the p-value was ≤ 0.05 of both the Quade omnibus-test and the post-hoc test and if the difference between the MFI ratios was ≤ 1 . Calculations were performed in R version 3.2.3.

Results

Parts of the following results were published in (Marti Fernandez et al. 2019)

8.1 Characterization of the glycosylation deficient mutants

It is unclear whether the increased binding to aglycosylated MOG by anti-MOG antibodies is due to the introduction of the negatively charged aspartate or due to the abrogation of glycosylation. To address this issue a neutral glycosylation deficient mutant of MOG (N31A) was generated (Marti Fernandez et al. 2019).

First, the aglycosylated MOG mutants were tested to confirm the lack of glycosylation. Lysates of cells transfected with wild type MOG or with the mutants, N31A and N31D, each fused to EGFP were treated with PNGaseF. Cell lysates were separated by SDS-PAGE, blotted and developed with anti-GFP mAb. PNGaseF treatment reduced the size of MOG while the sizes of the mutated variants N31A and N31D were not changed (Fig. 6A). This showed that N31A and N31D are not glycosylated and that N31 is the only N-linked glycosylation site used (Marti Fernandez et al. 2019).

Secondly, the MOG mutants were analysed for recognition by r8-18C5 using the cell-based assay, to see if the introduced mutations induced a gross alteration of MOG. We observed a similar expression and binding to r8-18C5 by both mutants compared to the wild-type MOG (Fig. 6B) (Marti Fernandez et al. 2019).

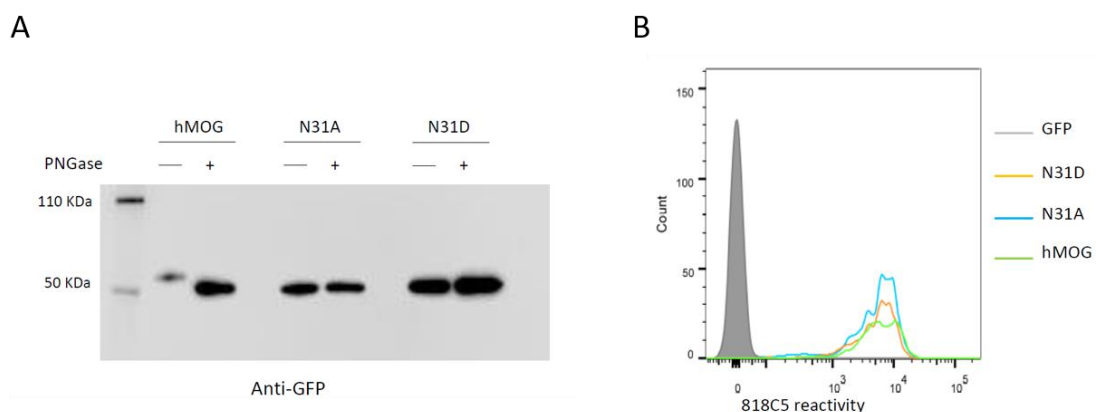


Figure 6: N31A and N31D mutations completely abrogate MOG glycosylation and have unaltered binding to r8-18C5. (A) Cell lysates of HeLa cells transiently transfected with the mutants N31A, N31D or wild-type MOG were digested with PNGase F as indicated. Subsequently, proteins were separated by SDS gel, blotted and developed with anti-GFP-HRP antibody. (B) HeLa cells were transfected with EGFP alone (closed gray graph), wild type MOG (green line), N31A (blue line) or N31D (orange line). Depicted is the reactivity of r8-18C5.

8.2 Heterogeneous response to two glycosylation deficient MOG mutants

27 anti-MOG positive patients (Table 1) were tested with wild-type MOG and two non-glycosylated variants of MOG, N31A and N31D in our cell-based assay. About 60 % of these patients (16/27) reacted to at least one of the two mutants different than to the wild type MOG. The raw data of the reactivity of each patient to each mutant are given in Table 7.

7 different patterns of reactivity towards the different non-glycosylated variants of MOG (Table 7 and Figure 7 and 8) were identified. In 11/27 patients there was no significant difference in recognition of these MOG mutants (Figure 7). In 7/27 patients a higher reactivity to both non-glycosylated MOG variants was observed, but since they showed further diversity on their recognition, they were classified in two different groups. Six of these 7 patients responded to the two mutants similarly (Figure 8A), while another one had a higher reactivity to N31D compared to N31A (# 15) (Figure 8B). In 5 other patients a higher reactivity to N31D than to wild-type MOG was observed, while the reactivity to N31A was not higher than to wild-type MOG (Figure 8C). Two patients (#12 and #13) showed an increased recognition of N31D, but had a reduced reactivity for the N31A (Figure 8D). An enhanced reactivity to N31A, but a reduced one to N31D was observed in one patient (#21) (Figure 8E). Patient #9 showed a reduced reactivity to N31A (Figure 8F) (Marti Fernandez et al. 2019).

Together, the reactivity to N31A was higher in 8/27 and lower in 3/27 patients, while the reactivity to N31D was higher in 14/27 and lower in only 1/27 patients. Looking at individual patients, this study reveals an enormous heterogeneity of human autoantibodies to MOG with 7 different patterns of recognition uncovered by two mutations of the MOG glycosylation site (Marti Fernandez et al. 2019).

Table 7. Heterogeneous response to two glycosylation deficient MOG mutants.

Patient ID	MFI ratio MOG	MFI ratio N31A	MFI ratio N31D	p-value WT vs N31A	p-value WT vs N31D	p-value N31A vs N31D
Similar reactivity						
2	6.0	7.4	5.6	0.506	0.506	1.000
4	29.0	34.2	32.9	0.506	0.506	1.000
6	211.2	164.3	199.9	0.297	1.000	0.297
10	142.4	138.3	168.5	0.574	0.083	0.188
16	187.2	225.0	211.1	0.622	0.203	0.399
18	3.7	3.9	4.6	0.390	0.060	0.214
20	5.7	7.7	7.7	0.049	0.058	0.910
23	3.7	3.6	4.4	0.064	0.039	0.003
25	97.5	114.4	117.6	0.058	0.049	0.910
26	132.5	103.9	133.7	0.161	0.781	0.108
27	77.5	86.7	121.2	0.897	0.227	0.190
Higher reactivity to N31A and N31D, but no difference between N31A and N31D						
1	9.1	16.8	18.9	0.022	0.008	0.500
7	2.6	6.0	5.3	0.002	0.034	0.034
8	44.3	70.5	90.1	0.047	0.017	0.473
11	93.2	124.7	117.4	0.008	0.022	0.500
17	27.9	89.9	56.5	0.002	0.025	0.112
19	5.9	7.5	8.2	0.024	0.005	0.337
Higher reactivity to N31A and N31D, and higher to N31D than to N31A						
15	9.8	13.9	47.4	0.034	0.002	0.034
Higher to N31D compared to WT and N31A						
3	28.5	28.0	36.6	0.325	0.022	0.005
5	80.6	77.0	108.3	0.894	0.013	0.017
14	28.9	30.6	40.7	0.500	0.008	0.022
22	45.8	42.0	102.8	0.112	0.025	0.002
24	14.5	14.4	18.9	0.337	0.024	0.005
Higher to N31D and lower to N31A						
12	38.8	31.4	70.1	0.034	0.034	0.002
13	94.2	65.7	102.1	0.034	0.034	0.002
Higher to N31A and lower to N31D						
21	15.1	45.5	7.7	0.034	0.034	0.002
Lower to N31A, but unaltered to N31D						
9	26.1	20.9	27.5	0.042	0.625	0.019

Mean fluorescence intensity (MFI) ratios were calculated as described in materials and methods; values represent the arithmetic mean of 4-5 experiments. Highlighted in grey are values considered significant. Patients (#20 and #25) had a p-value <0.05, but the response to the mutants was overall considered not significant since they did not pass the Omnibus test. Also, patients #7 and #23 had p values <0.05, but also these responses were not considered significant, because their differences of the MFI ratios were <1.

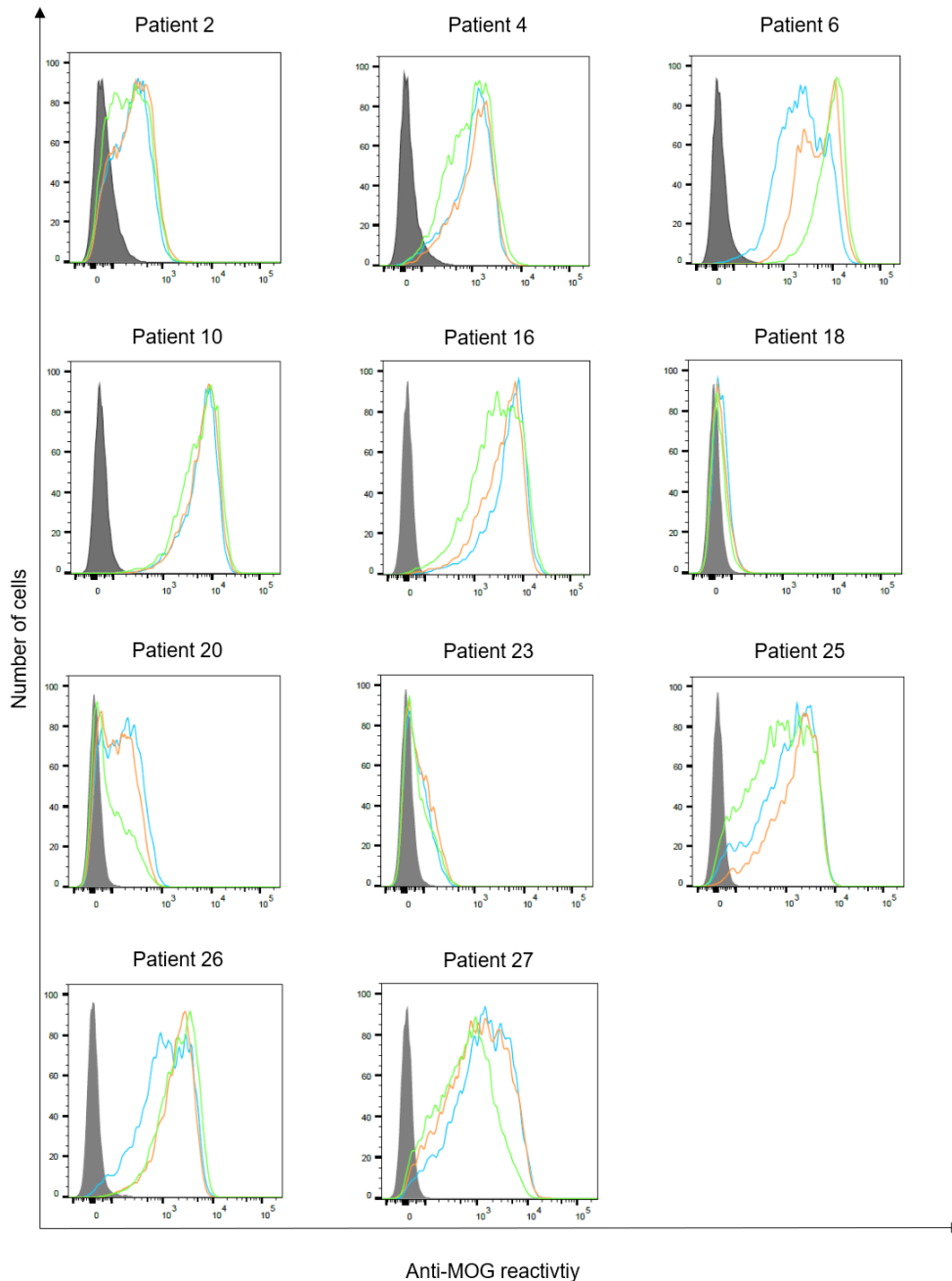


Figure 7: Patients with similar reactivities to MOG and both aglycosylated mutants, N31A and N31D (First pattern in table 7). HeLa cells were transfected with EGFP alone (closed gray graph), wild type MOG (green line), N31A (blue line) or N31D (orange line). Depicted is the reactivity of the 11 patients with no reactivity difference between the MOG variants. One representative experiment of 4-5 replicates is shown.

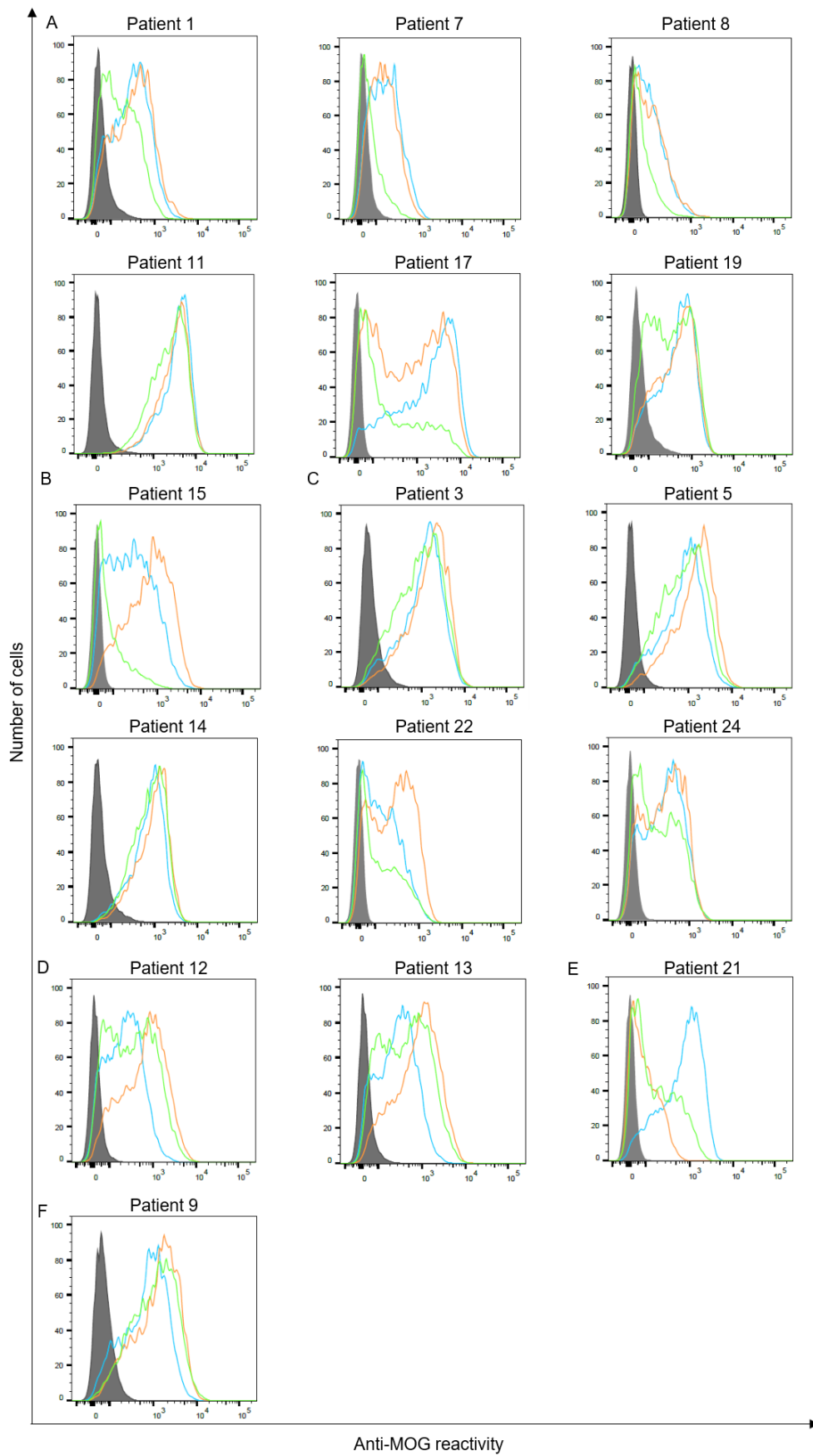


Figure 8: Six patterns of anti-MOG reactivity in patients to N31A and N31D (Patterns 2-7 in Table 7). HeLa cells were transfected with EGFP alone (closed gray graph), wild type MOG (green line), N31A (blue line) or N31D (orange line). One representative experiment of 4-5 replicates is shown. Whenever you use figures from your paper cite this in the legends

8.3 Purification of MOG and myelin glycoproteins

A recombinant version of the extracellular domain of human MOG was produced in HEK293-EBNA and the secreted extracellular domain of MOG was purified with a His Trap HP column. For the purification of myelin glycoproteins, myelin was obtained from a human healthy brain using a sucrose gradient and checked by western blot (Figure 9A). After the myelin was run through a lentil-lectin column to obtain the myelin glycoproteins out of the myelin, in order to enrich the amount of MOG in the preparation. Western blots were done in the myelin and in the myelin glycoproteins and MOG was detected only after the enrichment in the myelin glycoproteins portion, but not in the myelin (Figure 9B).

8.4 Glycoforms of MOG

MOG from HEK cells and myelin derived MOG were analysed by mass spectrometry. Glycoforms of MOG in HEK cells are important because HEK cells are the preferred expression system to analyse MOG-Abs in cell based-assays and determining the structure of myelin MOG could bring further insight in its role in antibody binding.

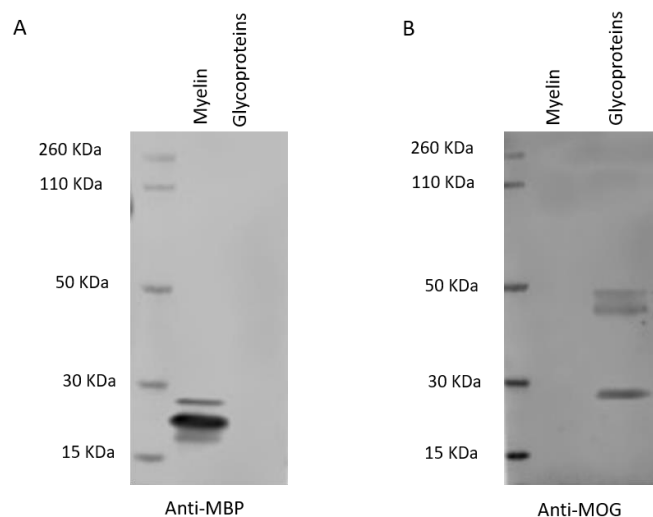


Figure 9: Purification of myelin and myelin glycoproteins from bovine brain. Myelin and myelin glycoproteins were obtained as indicated. Subsequently, proteins were separated by SDS gel, blotted and developed with anti-MBP or anti-MOG, respectively.

In-gel and in-solution enzymatic release of *N*-glycans from HEK derived MOG was performed. The sialic acid stabilized *N*-glycans were analyzed with MALDI-TOF-MS. A representative MS spectrum is shown in Figure 10A. To confirm the structural assignment, we subjected several *m/z* values to tandem mass spectrometry (MALDI-TOF/TOF-MS/MS, data not shown). For example, this proved informative with regard to antenna composition and fucosylation. Most spectra showed the presence of a core fucose, where the precursor showed a loss of the reducing end *N*-acetylglucosamine together with the fucose (367.2 Da). Antenna fucosylation was observed on both LacDiNAc and LacNAc antennae, resulting in the loss of 552.1 and 511.1 Da, respectively. Additionally, the presence of LacDiNAc was confirmed by the specific fragment at *m/z* 429.3. The MS/MS spectrum of the most abundant peak at *m/z* 2169.8 showed signal losses of 725.1 Da (LacDiNAc antenna carrying an α 2,6-linked sialic acid) and 684.3 Da (LacNAc antenna carrying an α 2,6-linked sialic acid). This indicated a mixture of two isomers, with the sialic acid either on the LacDiNAc or LacNAc antenna. In general, the presence of bisection of glycans could not be excluded (indicated with the white squares in Figure 10A and 10B) (Marti Fernandez et al. 2019).

In total 28 glycans were selected for relative quantification (Figure 10B). Most *N*-glycans were diantennary, with mainly LacNAc antennae as well as significant amounts of LacDiNAc antennae. The major glycans were sialylated species with predominantly 2,6-linked sialic acids. Most glycans showed core fucosylation, with some indications of additional antennary fucosylation. The glycan profiles obtained from in-solution and in-gel glycan release were highly consistent and showed only minor differences (Marti Fernandez et al. 2019).

Mass spectrometry was also performed in myelin derived MOG. As opposed as in the HEK derived MOG, we were only able to identify one glycoform on myelin MOG (Figure 10C). The glycan identified had a core fucose and a bisecting GlcNAc, furthermore there was an absence of sialic acids at the end of the glycan antennas. Further experiments are needed to confirm the myelin derived MOG glycoform.

and information from tandem MS spectra (data not shown). (B) Relative abundance of recombinant MOG released N-glycans. In total, 3 spots from and in-gel digestion and 4 spots from an in-solution release were analyzed. The graph shows the average relative abundances observed for 28 glycan species (normalized to the overall sum of intensities). Abbreviations used are hexose (H), N-acetylhexosamine (N), fucose (F) and N-acetylneuraminic acid with either α 2,3-linkage as indicated by lactonation (L) or α 2,6-linkage as indicated by esterification (E). Error bars: standard deviation. (C) MALDI-TOF-MS/MS of myelin glycoproteins. The glycan identified in the sample is shown (preliminary data). Figure taken from (Marti Fernandez et al. 2019)

9. Effector functions of wild-type mAb r8-18C5 and its variants

To address this issue, different variants of humanized r8-18C5 antibody (IgG1 isotype) with one or several mutations on their Fc parts were cloned and produced. Fc mutations were selected based on the literature (Ratelade et al. 2013; Khare et al. 2018; Lee et al. 2017; Gross et al. 2001) and they were always amino acids substitutions. Also, to better characterized the role of N-glycosylation on the Fc of antibodies, aglycosylated antibodies were used in this study. Aglycosylated antibodies were produced by disrupting the glycosylation sequence (Asn²⁹⁷-X²⁹⁸-Thr²⁹⁹, where X is any amino acid) with the substitution of Thr²⁹⁹ by Leu (Lee et al. 2017). On table 8 there is a summary of the different r8-18C5 variants with their mutations and their expected effector functions based on the literature.

Table 8: 8-18C5 mutants. r8-18C5 variants and their respective mutations.

Antibody	Mutation(s)	Expected effect	Reference
818C5	NONE	FcR and complement binding	Wild-type
T319L	T319L	Reduced FcR and complement binding	Glycosylation effect
G801	K340E;Q406R	Complement binding but No FcR binding	Lee et al, 2017. Nat.Immuno
A801	K340E;Q406R; T319L	Complement binding but No FcR binding	Lee et al, 2017. Nat.Immuno
G802	L255K;G256M; G257R;L371Q	No FcR or complement binding	Lee et al, 2017. Nat.Immuno
A802	L255K;G256M;G257R; L371Q;T319L	Complement binding but no FcR binding	Lee et al, 2017. Nat.Immuno
G803	A350S;P351S	Reduced FcR and complement binding	Atacicept, reduced C1q binding
A803	A350S;P351S; T319L	Reduced FcR and complement binding	Atacicept, reduced C1q binding
K342A	K342A	FcR binding but no complement binding	Khare et al, 2017. J. Autoimmun
AK342A	K342A;T319L	Reduced FcR and no complement binding	Khare et al, 2017. J. Autoimmun
G804	K346W;E353S	Enhanced complement but no FcR binding	Ratedale et al, 2013 Acta Neuropathol.

Antibodies were produced using HEK EBNA cells transfected with the mutated heavy chain and the wild-type light chain of the 8-18C5, then the supernatants were passed through a His Trap column. As an example, fractions of the purification of G804 antibody are shown in Figure 11. After purification, antibody concentration was measured using a BCA assay. It was not possible to produce three of these antibodies, because the antibodies were stored into the cells, instead of secreted into the culture medium, as shown by a western blot developed with an anti-IgG antibody. These antibodies are G802, A802 and AK342A, therefore they were not used in any of the experiments performed in this study.

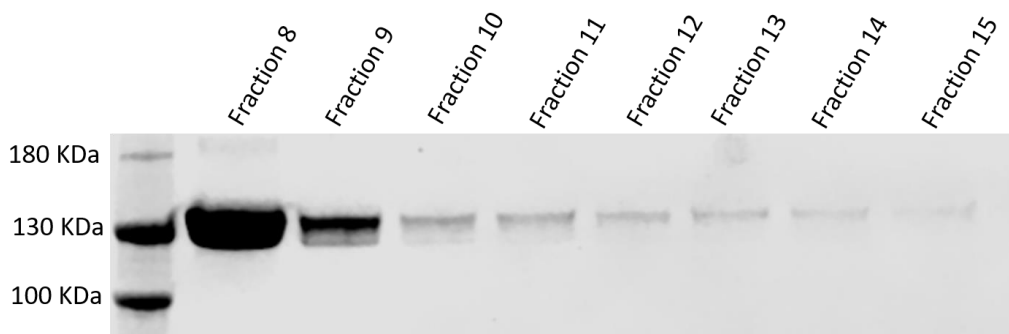


Figure 11: Fractions 8-15 of the His-Trap column for the G804 antibody purification. SDS-gel was loaded with 20µl of each fraction and stained with coomassie blue.

9.1 Characterization of the r8-18C5 mutants

After antibodies were produced, they were digested overnight with PNGaseF, in order to verify aglycosylated mutants were completely deglycosylated. Coomassie staining of the SDS-gels confirm that the mutants with the T299L substitution were completely aglycosylated (Figure 12).

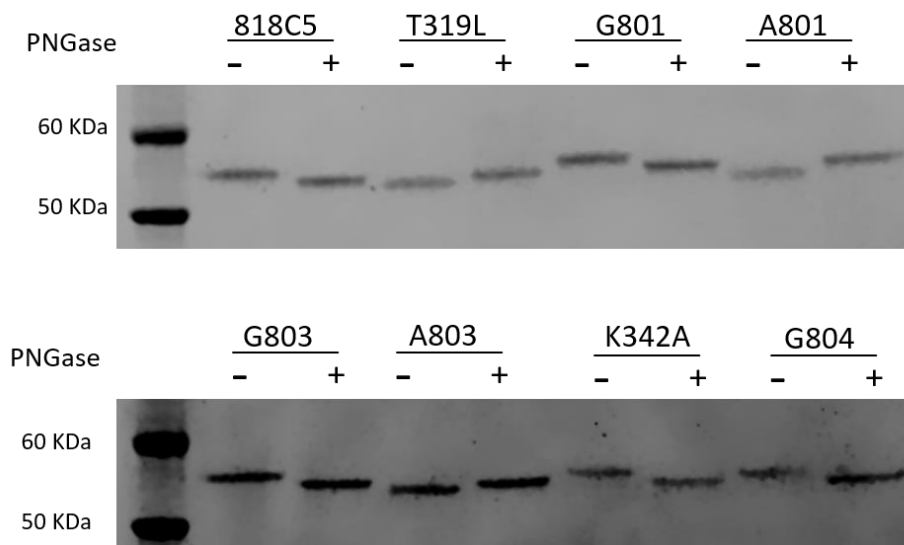


Figure 12: PNGaseF digestion of 8-18C5 variants. 100 µg of each antibody was digested with PNGaseF. 20 µg were loaded of each antibodies in a SDS gel and stained with coomassie blue.

Next, antibodies were tested for MOG-recognition using two different read outs, our cell-based assay and ELISA. For the cell-based assay HeLa cells were transfected with human MOG or EGFP (as a control) and incubated with the different r8-18C5 mutants (Figure 13A). In the case of the ELISA, biotinylated-MOG was coated to a streptavidin ELISA plate and then incubated with a serial dilution from 0.001 to 10 µg/ml of the antibodies (Figure 13B). All r8-18C5 variants were able to recognize human MOG similarly, even though a few of them (T319L, A801 and K342A antibodies) displayed a little less reactivity compared to the rest.

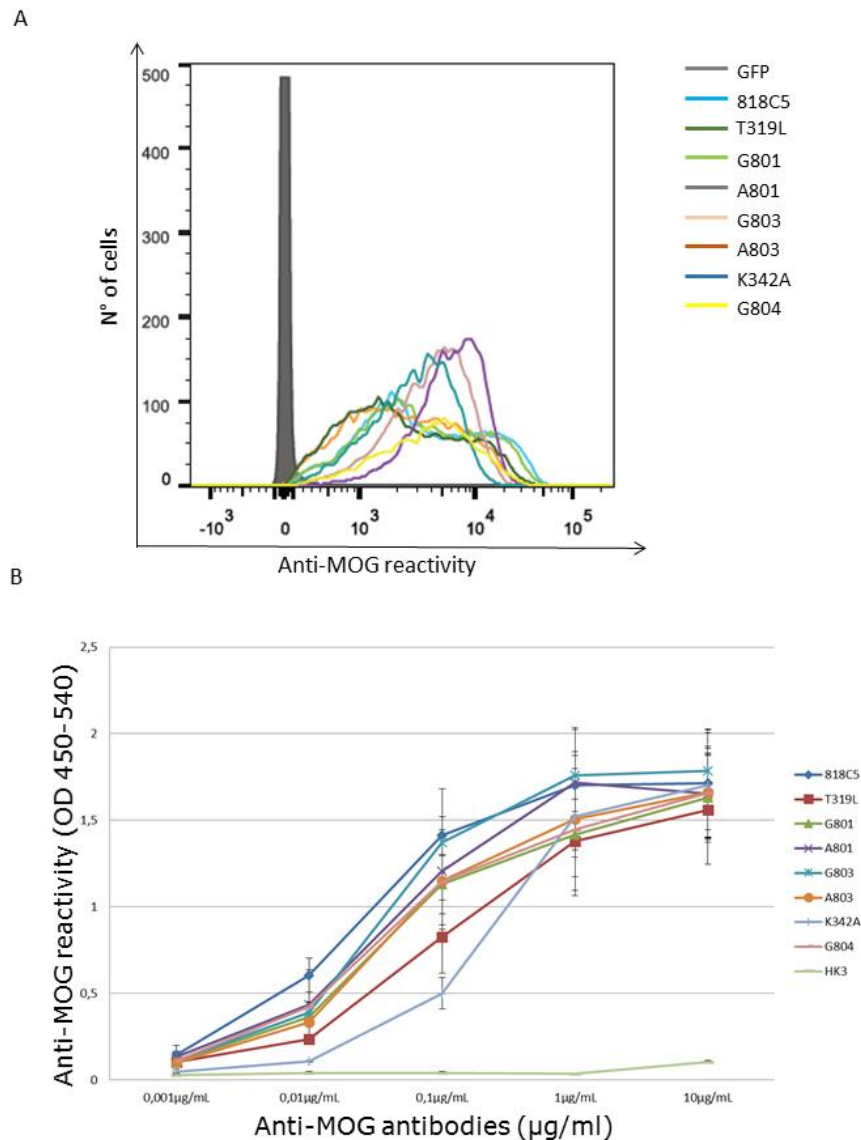


Figure 13: Binding of 8-18C5 mutants to human MOG. (A) r8-18C5 binding for MOG as measured by cell-based assay. HeLa cells were transfected with EGFP alone (closed gray graph) or wild type MOG. Two consecutive secondary antibodies were used, goat-anti-human IgG-biotin and Alexa fluor 647-streptavidin. One representative experiment of 3 replicates is shown. (B) Streptavidin ELISA depicting a serial dilution of the 8-18C5 variants (0.001 to 10 µg/ml) and their binding affinity to MOG. HK3 antibody is used as a negative control. Goat anti-human IgG-HRP was used as secondary antibody. The mean of 2 independent experiments is depicted, with the corresponding standard deviation.

The mutations introduced in the r8-18C5 variants are all located in the Fc part of the antibody. Therefore, the small differences observed on the binding to MOG by r8-18C5 variants, could be due to the binding of the secondary antibodies to the Fc part of the r8-18C5 mutants. To test this, the cell-based assay was performed with two different secondary antibodies, the usual one, goat anti-human IgG-biotin followed by incubation with Alexa-fluor 647-streptavidin, or using an anti-Histidine-peroxidase followed by incubation with anti-HRP Alexa Fluor® 647.

Similar binding was observed with the two different secondary antibodies, except in the case of the r8-18C5 and the G804 antibody (Figure 14). In the case of these two antibodies, the background of EGFP when using the anti-His antibody was really high, so the MFI ratio was lower compared to the anti-IgG binding. Despite that, this experiment showed that the differences observed when measuring the binding of the different r8-18C5 variants to MOG is not due to the mutations on their heavy chains.

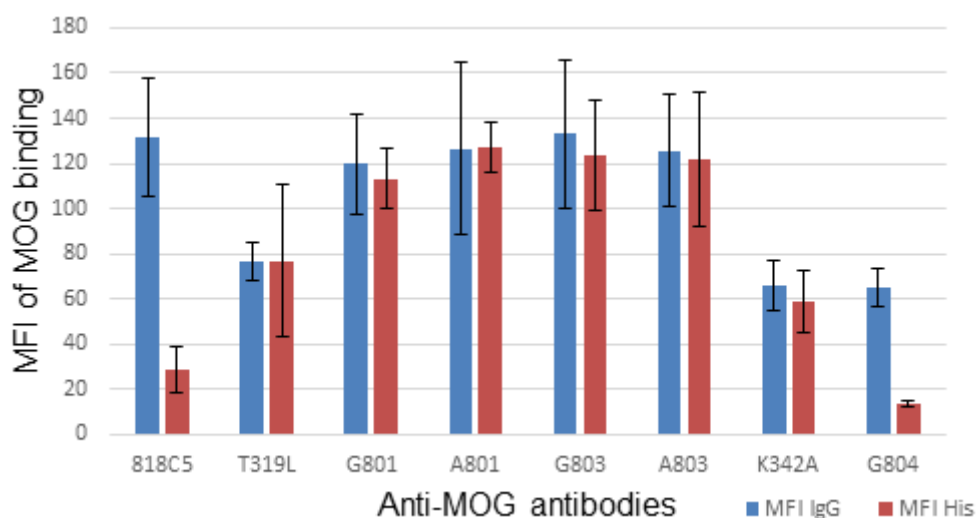


Figure 14: Comparison of IgG and anti-His antibodies. r8-18C5 binding for MOG as measured by cell-based assay. HeLa cells were transfected with EGFP alone (closed gray graph) or wild type MOG. Two consecutive secondary antibodies were used, goat-anti-human IgG-biotin and Alexa fluor 647-streptavidin (displayed in blue) or mouse anti-Histidine-peroxidase and anti-HRP Alexa fluor 647 (displayed in red). One representative experiment of 3 replicates is shown together with standard deviation. MFI (Mean fluorescent intensity)

9.2 Complement binding affinities of the r8-18C5 variants

Due to the mutations introduced in the Fc part of the r8-18C5 variants some of them were expected to have altered complement binding. According to the literature, mutants T319L, G803, A803, and K342A were expected to have a reduced or abolished complement binding. On the other hand, G804 antibody was expected to have an enhanced complement binding.

To test for the ability of r8-18C5 mutants to bind complement, their binding to C1q was measured by ELISA. The wild-type 8-18C5 was used as a reference and the HK3 antibody, which does not bind to MOG, was used as a negative control. As expected, G804 antibody and G801 had a comparable, and even higher affinity to C1q than the wild-type 8-18C5. Antibodies T319L, A803 and K342A had no binding to C1q and surprisingly, A801 and G803 antibodies had a reduced binding compared to wild-type 8-18C5. (Figure 15)

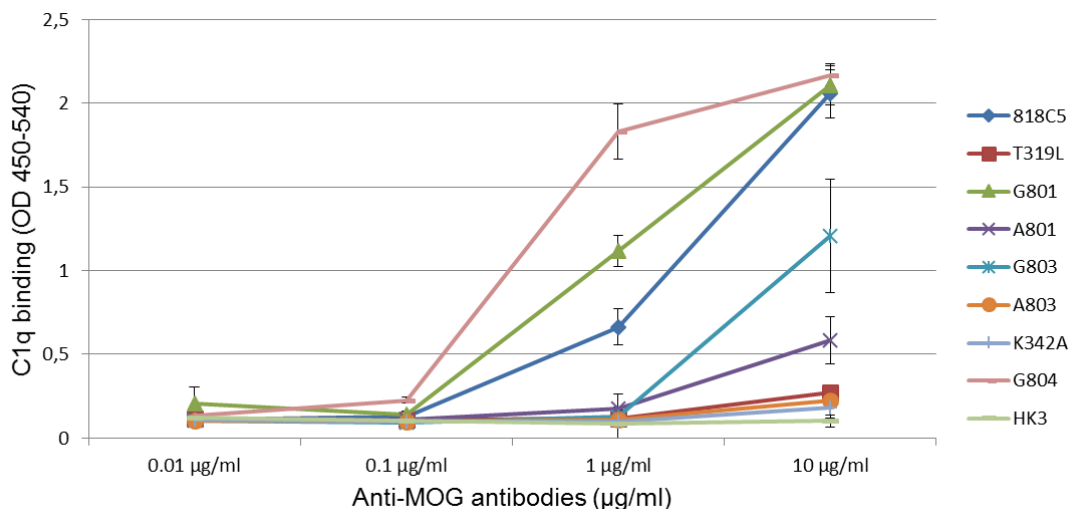


Figure 15: Binding of 8-18C5 mutants to human C1q. Streptavidin ELISA depicting a serial dilution of the 8-18C5 variants (0.001 to 10 µg/ml) and their binding affinity to C1q. HK3 antibody is used as a negative control. The mean of 2 independent experiments is depicted, with the corresponding standard deviation

9.3 mFcyRIII activation by r8-18C5 variants

8-18C5 variants were tested for their affinities to the mouse FcγRIII (m FcγRIII) using a reporter bioassay in which cells stably transfected with MOG (target cells) were incubated with Jurkat cells expressing mFcyRIII (effector cells) and the different 8-18C5 variants. If the 8-18C5 antibodies bind to mFcyRIII, luciferase signal was detected.

Antibodies were tested using mFcγRIII and not the human FcγRIII because in future experiments, the 8-18C5 variants will be tested in an EAE rat Lewis model to further understand the pathogenesis of EAE and MS development *in vivo*. mFcγRIII is of the activating mFcγR and is expressed in NK cells, dendritic cells and macrophages, among other cell types. Our 8-18C5 mutants are human IgG1 isotype and can activate bind to mFcγRIII and trigger the effector mechanisms.

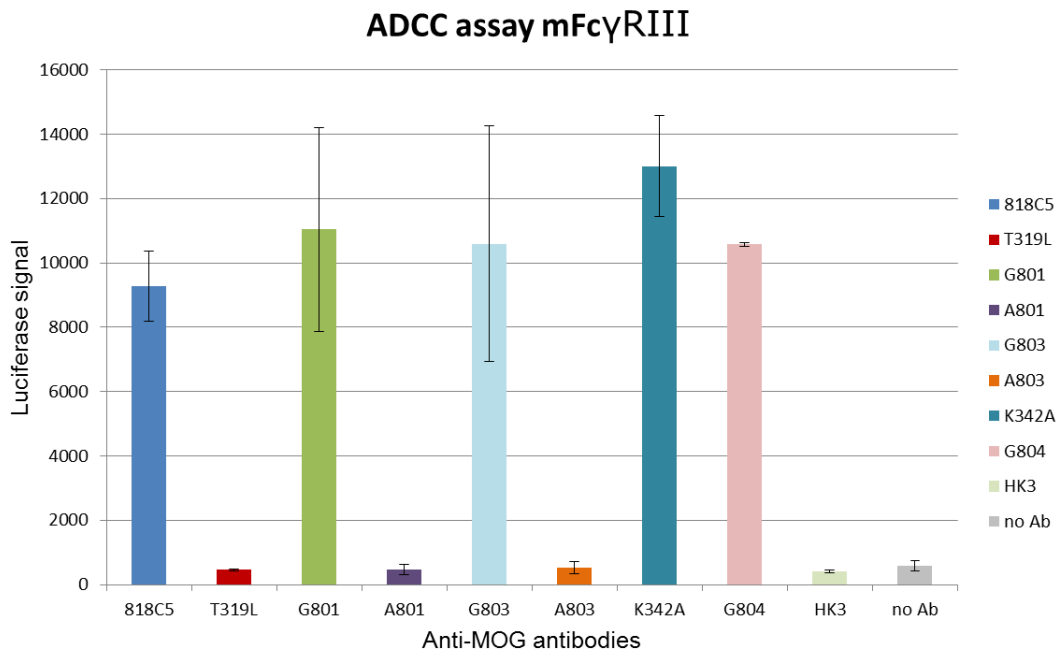


Figure 16: Activation of mFcγRIII by r8-18C5 variants. 25,000 cells expressing MOG were incubated with 75,000 effector cells and 5 µg/ml of the different antibodies for 12 hours. Luciferase signal was detected by luminescence detection. HK3 antibody was used as a negative control. The results of one of the experiments is depicted together with the corresponding SDs.

The reporter assay showed a range of activation of mFcγRIII. As expected, aglycosylated antibodies, T319L, A801 and A803 did not bind to mFcγRIII. On the other hand, the rest of the antibodies, G801, G803, K342A and G804 antibody showed the same or even higher reactivity for mFcγRIII than the wild-type 8-18C5 (Figure 16).

Table 9: Summary of 8-18C5 variants. Information regarding the glycosylation status, reactivity to MOG and their binding to C1q and mFcγRIII activation

Antibody	Mutation(s)	Glycosylation	MOG reactivity	C1q binding	FcRs activity
8-18C5	NONE	+	++	++	++
T319L	T319L	-	++	-	-
G801	K340E;Q406R	+	++	++	++
A801	K340E;Q406R;T319L	-	++	-	-
G803	A350S;P351S	+	++	+	++
A803	A350S;P351S;T319L	-	++	-	-
K342A	K342A	+	++	-	+++
G804	K346W;E353S	+	++	+++	++

Discussion

10. The glycosylation site of myelin oligodendrocyte glycoprotein affects autoantibody recognition in a large proportion of patients

This study revealed that the glycosylation site of MOG influences its recognition by autoantibodies in about 60% of patients. Two different glycosylation-deficient variants of MOG (N31D and N31A) were tested for their binding affinity by patients' autoantibodies and 7 different patterns of reactivity were observed. While previous studies had noted that the N31D mutant was stronger recognized by some patients (O'Connor et al. 2007; Mayer et al. 2013; Spadaro et al. 2015; Spadaro et al. 2016), the issue whether this is due to the introduced negative charge or due to the loss of the sugar part is still unknown. This project showed that both the negatively charged aspartate and the missing sugar can affect antigen recognition, in a different way in different patients (Marti Fernandez et al. 2019).

Specifically, 5 patients showed a higher reactivity to N31D, while the reactivity to N31A was the same as to the wild type. In two other patients a higher reactivity to N31D, but a lower one to N31A was observed. The conclusion was that in these patients the introduced negative charge is responsible for the enhanced binding to MOG rather than the absence of the glycan (Marti Fernandez et al. 2019).

In 7 other patients, there was a stronger reactivity to both N31D and N31A. Six of these patients showed a similarly enhanced reactivity to both mutants, while one recognized N31D stronger than N31A. One further patient showed a higher reactivity to N31A, but even a lower one to N31D. In these 7/27 patients with an enhanced reactivity to N31A the glycan on MOG provides a hindrance for antibody binding, reminding of the impact of the glycan shield of HIV and SIV (Reitter, Means, and Desrosiers 1998; Wei et al. 2003; Marti Fernandez et al. 2019).

Furthermore, the MOG-reactivity of these patients is heterogeneous concerning the impact of the negatively charged N31D. One out of 27 patients showed a slightly lower reactivity to N31A, but still a clear reactivity to this glycosylation-deficient mutant. Thus, in this patient, the glycan on MOG might slightly enhance its binding to the protein-backbone. The observation that the prototype anti-MOG r8-18C5 was not affected by any of the glycosylation deficient mutants is in accordance with the previous reports (Breithaupt et al. 2003; Mayer et al. 2013). The identification of 7 different patterns of

reactivity just using different mutations of the glycosylation site extends the knowledge about heterogeneity of MOG-epitopes recognized by patient antibodies. Those patients who show a different reactivity to N31D and/or N31A might directly recognize the BC-loop of MOG, where the *N*-linked glycosylation site is located (Mayer et al. 2013), but the possibility that mutations of N31 of MOG have far-reaching effects on other parts of MOG with an impact on antibody binding at a remote side cannot be excluded. An example for an alteration of protein-protein bindings remote from the mutation site, is the recent observation that a variant of alpha-1 antitrypsin at one side (aa213) affects the interaction of a remote part of the molecule (aa143-153) with the enzyme it inhibits, neutrophil elastase (Malik et al. 2017; Marti Fernandez et al. 2019).

These findings indicate that this glycan structure can provide a steric hindrance for antibody binding; this might have implications for further improvement of assays to detect MOG antibodies suggesting that the use of a neutral glycosylation-deficient MOG mutant (like N31A) would enhance the sensitivity to detect autoantibodies to MOG. In none of the patients the reactivity to MOG depended on the glycan structure, clearly different than it was described for recognition of contactin, where some patients' autoantibodies have a higher reactivity for contactin depending on the glycoforms present on the protein (Labasque et al. 2014) (Marti Fernandez et al. 2019).

Glycans regulate protein-protein interactions. In an intriguing paper, glycosylation of MOG on myelin has been linked to binding to DC-SIGN and a role for myelin glycosylation in immune homeostasis of the healthy CNS was shown (Garcia-Vallejo et al. 2014). That study further showed that removal of fucose from myelin reduced the DC-SIGN-dependent homeostatic control of myelin (Garcia-Vallejo et al. 2014). Thus, identifying the glycan structures on MOG might help to further study how MOG interacts with relevant proteins involved in the inflammatory process.

The glycan structures of MOG produced in HEK cells and myelin derived MOG were determined by mass spectrometry. In HEK cells, the most abundant glycoforms in MOG are diantennary, contain a core fucose, an antennary fucose and are decorated with α 2,6 linked Neu5Ac. On the other hand, the glycan identified in myelin derived MOG had a core fucose and a bisecting GlcNac, and there was an absence of sialic acids at the end of the glycan antennas. In addition, a previous study reported that the majority of myelin MOG glycans have one or two terminal fucoses, corresponding to the Lewis-type structures (Garcia-Vallejo et al. 2014). A couple of the glycans identified in HEK cells could contain a terminal fucose, but no terminal fucoses or sialic acids were detected in myelin derived MOG.

The differences on the glycan structures observed between HEK and myelin derived MOG are expected since they come from different cell types and each cell type is able to produce different glycan structures (Goh and Ng 2018). In addition, the differences might be partially attributed to the different purification methods. HEK derived MOG was purified using a His Trap column and myelin-derived MOG was purified by enriching the myelin glycoproteins fraction of the myelin using a Lentil-Lectin column, which has a high preference for glycans with mannose and glucose, which can create a bias in the MOG glycan that was detected by mass spectrometry.

As mentioned, the glycan structure of myelin derived MOG is preliminary and further experiments are needed to confirm it. A possibility to avoid the bias on the Lentil-lectin column could be to pass the myelin through a protein G column, previously coated with 8-18C5 antibody. It would be of interest to further analyse the glycan of myelin derived MOG to determine the presence of sialic acids, like the ones observed in HEK cells. If this is confirmed, future research could analyse whether MOG also interacts with sialic acid binding proteins such as Siglecs (sialic acid-binding immunoglobulin like lectins) (Macauley, Crocker, and Paulson 2014).

11. r8-18C5 variants and their effector functions

MOG-Abs from patients are pathogenic by two mechanisms, demyelination and enhancement of the activation of cognate T cells, but the linkage of Fc effector functions to these pathomechanisms is unclear. In this part of the thesis, different clones of the humanized 8-18C5 antibody were constructed and characterized for C1q binding and FcR activation. These mutants were picked due to previous studies, but the results obtained were not always in accordance to them. In table 9 there is a summary of the properties of the generated 8-18C5 variants.

All mutants were able to recognize MOG in our cell-based assay as well as in ELISA, although there were slight differences in their binding affinities to MOG. Then, the ability of the 8-18C5 variants was tested for their ability to bind to C1q in an ELISA and the capacity of the antibodies to activate mFcγRIII.

The antibody G801 was able to bind to C1q as expected, but on the other hand, it was also able to activate mFcγRIII with high affinity. A previous study showed that the mutations on clone G801 were able to abolish the binding to all human FcγR and it just bound weakly to the high affinity human FcγRI (Lee et al. 2017). Here, mFcγRIII, instead of human FcγR was used, but it has been shown that human IgG have similar affinities to both, human and mouse FcγRs (Dekkers et al. 2017), so such a high binding to

mFcγRIII was surprising. They performed an X-ray analysis of the Fc structure of G801 and found that the two FcγR-binding subsites of G801-Fc (one is centred near the C'E loop of one chain and the hinge LLPP motif of the other) were sterically accessible, however, they seemed to be highly flexible and /or disordered (Lee et al. 2017). This Fc structure could explain why G801 is able to bind to mFcγRIII, since the FcγR-binding sites are still accessible despite the mutations introduced. Alternatively, the differences observed could be due to the method used for assessing the capability of G801 to activate FcγRs. They used a binding competition assay and flow cytometry to determine that the antibody did not activate to FcγRs and they further tested the antibody ability to mediate cell death using an ADCC assay (Lee et al. 2017). In this thesis, a bioassay to determine the activation of mFcγRIII by the 8-18C5 antibody variants was used, and luciferase signal was the read out. In the case of the G804 antibody, as previously observed it had a higher affinity for complement binding compared to wild-type 8-18C5, but unexpectedly it also bound to mFcγRIII. An explanation for this difference could be in the methodology used to study the activation of FcγRs. They assessed its ability to recognize FcγRs by doing an ADCC experiment and using cell death as a read-out system (Ratelade et al. 2013). Their experiment also used target and effector cells, but they measured cell-death and here, activation of mFcγRIII and not cell death was determined. Further replicates for the binding to the mFcγRIII by 8-18C5 variants are needed as well as other experiments, such as measuring the binding affinity to all mFcγRs by FACS or ELISA.

G803 and K342A antibodies bound to C1q and mFcγRIII as expected according to previous research reports (Gross et al. 2001; Khare et al. 2018). G803 contain the same two mutations that Atacicept, a recombinant protein that inhibits B cell proliferation and has five mutations, two of which also has the G803 antibody and are meant to abolish or reduce complement binding (Gross et al. 2001) The G803 clone displayed reduced affinity for complement compared to 8-18C5. Previous studies found that binding to C1q could overestimate the actual CDC activity, since IgG clustering enhance C1q binding and may always be a perfect read-out system for complement activation (Phuan et al. 2012). The two mutations present in this antibody are near the sites that mediate FcγRs binding (Gross et al. 2001), and they can also have an effect on FcγRs activation, but this was not the case in our read-out system, since G803 could activate mFcγRIII as good as 8-18C5. On the other hand, K342A antibody mutation is known to abolish complement binding (Khare et al. 2018) but preserve FcγRs binding (Shields et al. 2001) and these findings were confirmed in this study .

Due to the relevance of Fc-glycosylation, here three aglycosylated antibody mutants were tested. T319L, A801 and A803 had a reduced or completely abolished binding for complement and FcγRs as is expected from aglycosylated antibodies (Nimmerjahn and Ravetch 2008). In the case of the A801, even if it is an aglycosylated IgG, a previous study reported that this antibody had the ability to highly bind to C1q and it was also able to kill cells by CDC (Lee et al. 2017). In the same study, they determined the X-ray Fc-structure of A801 and concluded that the reason why this specific aglycosylated antibody is able to bind and activate the complement cascade was due to the conformational flexibility of its CY2 region (Lee et al. 2017). In the same line, there is another study that showed that removing of the glycan in Asn²⁹⁷ increases the conformational flexibility of CY2 and that this flexibility could contribute to the binding of A801 to C1q (Borrok et al. 2012; Lee et al. 2017). Despite this, here the A801 antibody performed as expected from an aglycosylated IgG in the C1q ELISA and in the mFcγRIII activation bioassay.

Another possibility to explain the differences between the results obtained in this thesis and previous studies is the modulatory effect of the Fab region. Earlier studies showed that the interaction between the Fab and Fc regions can affect the effector mechanisms of the antibody. For example, a study suggested that Fab arms affected C1q binding by a steric obstruction of the C1q-binding sites on the Fc region (Isenman, Dorrington, and Painter 1975). In the same line, another paper observed that activation of FcγRs by the Fc region could be impaired by Fab through conformational changes or by obscuring the putative FcγRs-binding sites in Fc (Birshtein, Campbell, and Diamond 1982). Recently, using High-speed atomic force microscopy and hydrogen/deuterium exchange mass spectrometric analysis, a study revealed that the Fab portion of IgG has putative FcγRIIIa-binding sites, indicating that the Fab region is directly involved in the interaction with FcγRIIIa (Yogo et al. 2019).

Further experiments are needed to better characterize these 8-18C5 antibodies and determine not only their binding capabilities *in vitro*, but also to observe if they are able to trigger CDC and ADCC *in vivo*. These experiments are important in order to decide which antibody variants would be injected in an EAE rat Lewis model to get further insight in the pathogenesis of MS and related disorders. Also, 8-18C5 variants could have a potential therapeutic effect. A pathogenic antibody targeting AQP4, unable to perform CDC or ADCC, competed for binding with pathogenic antibodies and therefore, prevented the formation of NMO lesions in spinal cord slice cultures and in mice (Tradtrantip et al. 2012). The same approach could be used with the 8-18C5 variants in order to avoid the formation of brain lesions in patients with anti-MOG antibodies.

Conclusions

This study showed the importance of the glycosylation site of MOG for binding of autoantibodies in a large proportion of patients. The finding that the glycan provides a hindrance for antibody binding in a proportion of patients has implications for development of assays to enhance the sensitivity to detect antibodies to MOG. Here, seven different patterns of MOG-binding to glycosylation-deficient variants were observed and provided further insight into details of antigen-recognition and extended the known heterogeneity of human autoantibodies against MOG.

Moreover, the 8-18C5 variants cloned in this project can be used to get a better understanding on how MOG autoantibodies trigger disease pathology and if there is any predominant effector function in MS and related CNS demyelinating disorders. These newly developed antibodies could be used in future therapeutic approaches, where they compete with autoantibodies from the patients to prevent the formation of brain lesions.

References

- Abdul-Majid, KB, A Stefferl, C Bourquin, H Lassmann, C Linington, T Olsson, S Kleinau, and RA Harris. 2002. 'Fc receptors are critical for autoimmune inflammatory damage to the central nervous system in experimental autoimmune encephalomyelitis.', *Scand J Immunol*, 55: 70-81.
- Adelmann, M, J Wood, I Benzel, P Fiori, H Lassmann, JM Matthieu, MV Gardinier, K Dornmair, and Linington C. 1995. 'The N-terminal domain of the myelin oligodendrocyte glycoprotein (MOG) induces acute demyelinating experimental autoimmune encephalomyelitis in the Lewis rat.', *J Neuroimmunol*, 63: 17-27.
- Agius, MA, G2 Klodowska-Duda, M Maciejowski, A Potemkowski, J Li, K Patra, J Wesley, S Madani, G Barron, E Katz, and A Flor. 2019. 'Safety and tolerability of inebilizumab (MEDI-551), an anti-CD19 monoclonal antibody, in patients with relapsing forms of multiple sclerosis: Results from a phase 1 randomised, placebo-controlled, escalating intravenous and subcutaneous dose study.', *Mult Scler.*, 25: 235-45.
- Arnold, JN, MR Wormald, RB Sim, PM Rudd, and RA Dwek. 2007. 'The impact of glycosylation on the biological function and structure of human immunoglobulins.', *Annu Rev Immunol.*, 25: 21-50.
- Bennett, Jeffrey L., Chiwah Lam, Sudhakar Reddy Kalluri, Philippe Saikali, Katherine Bautista, Cecily Dupree, Magdalena Glogowska, David Case, Jack P. Antel, Gregory P. Owens, Don Gilden, Stefan Nessler, Christine Stadelmann, and Bernhard Hemmer. 2009. 'Intrathecal pathogenic anti-aquaporin-4 antibodies in early neuromyelitis optica', *Ann Neurol.*, 66: 617-29.
- Birshtein, B. K., R. Campbell, and B. Diamond. 1982. 'Effects of immunoglobulin structure on Fc receptor binding: a mouse myeloma variant immunoglobulin with a gamma 2b-gamma 2a hybrid heavy chain having a complete gamma 2a Fc region fails to bind to gamma 2a Fc receptors on mouse macrophages.', *J Immunol.*, 129: 610-14.
- Borrok, M. Jack, Sang Taek Jung, Tae Hyun Kang, Arthur F. Monzingo, and George Georgiou. 2012. 'Revisiting the Role of Glycosylation in the Structure of Human IgG Fc', *ACS Chem Biol.*, 7: 1596-602.
- Bourquin, C., A. Schubart, S. Tobollik, I. Mather, S. Ogg, R. Liblau, and C. Linington. 2003. 'Selective Unresponsiveness to Conformational B Cell Epitopes of the Myelin Oligodendrocyte Glycoprotein in H-2b Mice', *J Immunol.*, 171: 455-61.
- Bradl, Monika, Tatsuro Misu, Toshiyuki Takahashi, Mitsutoshi Watanabe, Simone Mader, Markus Reindl, Milena Adzemovic, Jan Bauer, Thomas Berger, Kazuo Fujihara, Yasuto Itoyama, and Hans Lassmann. 2009. 'Neuromyelitis optica: Pathogenicity of patient immunoglobulin in vivo', *Ann Neurol.*, 66: 630-43.
- Breithaupt, C., A. Schubart, H. Zander, A. Skerra, R. Huber, C. Linington, and U. Jacob. 2003. 'Structural insights into the antigenicity of myelin oligodendrocyte glycoprotein', *Proc Natl Acad Sci U S A*, 100: 9446-51.
- Brilot, Fabienne, Russell C. Dale, Rebecca C. Selter, Verena Grummel, Sudhakar Reddy Kalluri, Muhammad Aslam, Verena Busch, Dun Zhou, Sabine Cepok, and Bernhard Hemmer. 2009. 'Antibodies to native myelin oligodendrocyte glycoprotein in children with inflammatory demyelinating central nervous system disease', *Ann Neurol.*, 66: 833-42.
- Bruhns, P. 2018. 'Properties of mouse and human IgG receptors and their contribution to disease models', *Blood.*, 19: 5640-49.
- Brunner, C, H Lassmann, TV Waehneltd, JM Matthieu, and C Linington. 1989. 'Differential ultrastructural localization of myelin basic protein, myelin/oligodendroglial

- glycoprotein, and 2',3'-cyclic nucleotide 3'-phosphodiesterase in the CNS of adult rats.', *J Neurochem.*, 52: 296-304.
- Burger, D, AJ Steck, CC Bernard, and N Kerlero de Rosbo. 1993. 'Human myelin/oligodendrocyte glycoprotein: a new member of the L2/HNK-1 family.', *J Neurochem.*, 61: 1822-7.
- Clements, C. S., H. H. Reid, T. Beddoe, F. E. Tynan, M. A. Perugini, T. G. Johns, C. C. A. Bernard, and J. Rossjohn. 2003. 'The crystal structure of myelin oligodendrocyte glycoprotein, a key autoantigen in multiple sclerosis', *Proc Natl Acad Sci U S A.*, 100: 11059-64.
- Dekkers, Gillian, Arthur E. H. Bentlage, Tamara C. Stegmann, Heather L. Howie, Suzanne Lissenberg-Thunnissen, James Zimring, Theo Rispens, and Gestur Vidarsson. 2017. 'Affinity of human IgG subclasses to mouse Fc gamma receptors', *mAbs*, 9: 767-73.
- Delarasse, Cécile, Philippe Daubas, Lennart T. Mars, Csaba Vizler, Tobias Litzenburger, Antonio Iglesias, Jan Bauer, Bruno Della Gaspera, Anna Schubart, Laurence Decker, Dalia Dimitri, Guy Roussel, Andrée Dierich, Sandra Amor, André Dautigny, Roland Liblau, and Danielle Pham-Dinh. 2003. 'Myelin/oligodendrocyte glycoprotein-deficient (MOG-deficient) mice reveal lack of immune tolerance to MOG in wild-type mice', *J Clin Invest.*, 112: 544-53.
- Di Pauli, Franziska, and Thomas Berger. 2018. 'Myelin Oligodendrocyte Glycoprotein Antibody-Associated Disorders: Toward a New Spectrum of Inflammatory Demyelinating CNS Disorders?', *Front Immunol*, 9: 2753.
- Duncan, AR, and G Winter. 1988. 'The binding site for C1q on IgG.', *Nature*, 332: 738-40.
- Flach, Anne-Christine, Tanja Litke, Judith Strauss, Michael Haberl, César Cordero Gómez, Markus Reindl, Albert Saiz, Hans-Jörg Fehling, Jürgen Wienands, Francesca Odoardi, Fred Lühder, and Alexander Flügel. 2016. 'Autoantibody-boosted T-cell reactivation in the target organ triggers manifestation of autoimmune CNS disease', *Proc Natl Acad Sci U S A.*, 113: 3323-28.
- Garcia-Vallejo, J. J., J. M. Ilarregui, H. Kalay, S. Chamorro, N. Koning, W. W. Unger, M. Ambrosini, V. Montserrat, R. J. Fernandes, S. C. Bruijns, J. R. van Weering, N. J. Paauw, T. O'Toole, J. van Horssen, P. van der Valk, K. Nazmi, J. G. Bolscher, J. Bajramovic, C. D. Dijkstra, B. A. t Hart, and Y. van Kooyk. 2014. 'CNS myelin induces regulatory functions of DC-SIGN-expressing, antigen-presenting cells via cognate interaction with MOG', *J Exp Med*, 211: 1465-83.
- Gardinier, MV, and JM Matthieu. 1993. 'Cloning and cDNA sequence analysis of myelin/oligodendrocyte glycoprotein: a novel member of the immunoglobulin gene superfamily.', *Schweiz Arch Neurol Psychiatr*, 144: 201-7.
- Genain, C. P., M. H. Nguyen, N. L. Letvin, R. Pearl, R. L. Davis, M. Adelman, M. B. Lees, C. Linington, and S. L. Hauser. 1995. 'Antibody facilitation of multiple sclerosis-like lesions in a nonhuman primate', *J Clin Invest.*, 96: 2966-74.
- Goh, Justin Bryan, and Say Kong Ng. 2018. 'Impact of host cell line choice on glycan profile', *Crit Rev Biotechnol*, 38: 851-67.
- Gross, Jane A., Stacey R. Dillon, Sherri Mudri, Janet Johnston, Alisa Littau, Richard Roque, Mark Rixon, Ole Schou, Kevin P. Foley, Harald Haugen, Susan McMillen, Kim Waggie, Randy W. Schreckhise, Kim Shoemaker, Tuyen Vu, Margaret Moore, Angelika Grossman, and Chris H. Clegg. 2001. 'TACI-Ig Neutralizes Molecules Critical for B Cell Development and Autoimmune Disease', *Immunity.*, 15: 289-302.
- Hart, Bert A. 'T, Jon D. Laman, Jan Bauer, Erwin Blezer, Yvette Van Kooyk, and Rogier Q. Hintzen. 2004. 'Modelling of multiple sclerosis: lessons learned in a non-human primate', *Lancet Neurol.*, 3: 588-97.
- Hauser, Stephen L., Emmanuelle Waubant, Douglas L. Arnold, Timothy Vollmer, Jack Antel, Robert J. Fox, Amit Bar-Or, Michael Panzara, Neena Sarkar, Sunil Agarwal, Annette Langer-Gould, and Craig H. Smith. 2008. 'B-Cell Depletion with Rituximab in Relapsing-Remitting Multiple Sclerosis', *New Engl J Med*, 358: 676-88.

- Heigl, Franz, Reinhard Hettich, Rainer Arendt, Joachim Durner, Jürgen Koehler, and Erich Mauch. 2013. 'Immunoabsorption in steroid-refractory multiple sclerosis: Clinical experience in 60 patients', *Atheroscler Suppl.*, 14: 167-73.
- Hess, Christoph, and Claudia Kemper. 2016. 'Complement-Mediated Regulation of Metabolism and Basic Cellular Processes', *Immunity*, 45: 240-54.
- Hickman, SJ, CM Dalton, DH Miller, and Plant GT. 2002. 'Management of acute optic neuritis.', *Lancet*, 360: 1953-62.
- Hoffmann, Franziska, and Edgar Meinl. 2014. 'B cells in Multiple Sclerosis: Good or bad guys?', *Eur J Immunol.*, 44: 1247-50.
- Hohlfeld, Reinhard, Klaus Dornmair, Edgar Meinl, and Hartmut Wekerle. 2016. 'The search for the target antigens of multiple sclerosis, part 2: CD8+ T cells, B cells, and antibodies in the focus of reverse-translational research', 15: 317-31.
- Ishemura, D. E., K. J. Dorrington, and R. H. Painter. 1975. 'The structure and function of immunoglobulin domains. II. The importance of interchain disulfide bonds and the possible role of molecular flexibility in the interaction between immunoglobulin G and complement.', *J Immunol.*, 114: 1726-29.
- Jacob, A., A. McKeon, I. Nakashima, D. K. Sato, L. Elson, K. Fujihara, and J. De Seze. 2013. 'Current concept of neuromyelitis optica (NMO) and NMO spectrum disorders', *J Neurol Neurosurg Psychiatry.*, 84: 922-30.
- Jarius, S., I. Metz, B. F. K. Ruprecht, M. Reindl, F. Paul, W, and B. Wildemann. 2016. 'Screening for MOG-IgG and 27 other anti-glial and anti-neuronal autoantibodies in 'pattern II multiple sclerosis and brain biopsy findings in a MOG-IgG-positive case', *Mult Scler.*, 22: 1541-49.
- Jarius, S., F. Paul, O. Aktas, N. Asgari, R. C. Dale, J. De Seze, D. Franciotta, K. Fujihara, A. Jacob, H. J. Kim, I. Kleiter, T. Kümpfel, M. Levy, J. Palace, K. Ruprecht, A. Saiz, C. Trebst, B. G. Weinshenker, and B. Wildemann. 2018. 'MOG encephalomyelitis: international recommendations on diagnosis and antibody testing', *J Neuroimmunol*, 15: 134.
- Johns, TG, and CC Bernard. 1997. 'Binding of complement component C1q to myelin oligodendrocyte glycoprotein: a novel mechanism for regulating CNS inflammation.', *Mol Immunol.*, 34: 33-8.
- Jurynczyk, M., S. Messina, M. R. Woodhall, N. Raza, R. Everett, A. Roca-Fernandez, G. Tackley, S. Hamid, A. Sheard, G. Reynolds, S. Chandratre, C. Hemingway, A. Jacob, A. Vincent, M. I. Leite, P. Waters, and J. Palace. 2017. 'Clinical presentation and prognosis in MOG-antibody disease: a UK study', *Brain*, 140: 3128-38.
- Kabat, Elvin A., Dan H. Moore, and Harold Landow. 1942. 'An electrophoretic study of the protein components in cerebrospinal fluid and their relationship to the serum proteins', *J Clin Invest.*, 21: 571-77.
- Kao, Daniela, Heike Danzer, Mattias Collin, Andrea Groß, Jutta Eichler, Jerko Stambuk, Gordan Lauc, Anja Lux, and Falk Nimmerjahn. 2015. 'A Monosaccharide Residue Is Sufficient to Maintain Mouse and Human IgG Subclass Activity and Directs IgG Effector Functions to Cellular Fc Receptors', *Cell Rep.*, 13: 2376-85.
- Kappos, Ludwig, David Li, Peter A. Calabresi, Paul O'Connor, Amit Bar-Or, Frederik Barkhof, Ming Yin, David Leppert, Robert Glanzman, Jeroen Tinbergen, and Stephen L. Hauser. 2011. 'Ocrelizumab in relapsing-remitting multiple sclerosis: a phase 2, randomised, placebo-controlled, multicentre trial', *Lancet.*, 378: 1779-87.
- Keegan, M, F König, R McClelland, W Brück, Y Morales, A Bitsch, H Panitch, H Lassmann, B Weinshenker, M Rodriguez, J Parisi, and CF Lucchinetti. 2005. 'Relation between humoral pathological changes in multiple sclerosis and response to therapeutic plasma exchange.', *Lancet.*, 366: 579-82.
- Khare, Priyanka, Dilip K. Challa, Siva Charan Devanaboyina, Ramraj Velmurugan, Samuel Hughes, Benjamin M. Greenberg, Raimund J. Ober, and E. Sally Ward. 2018. 'Myelin

- oligodendrocyte glycoprotein-specific antibodies from multiple sclerosis patients exacerbate disease in a humanized mouse model', *J Autoimmun*, 86: 104-15.
- Kinoshita, M, Y Nakatsuji, T Kimura, M Moriya, K Takata, T Okuno, A Kumanogoh, K Kajiyama, H Yoshikawa, and Sakoda S. 2009. 'Neuromyelitis optica: Passive transfer to rats by human immunoglobulin.', *Biochem Biophys Res Commun*, 386: 623-7.
- Kinzel, Silke, Klaus Lehmann-Horn, Sebastian Torke, Darius Häusler, Anne Winkler, Christine Stadelmann, Natalie Payne, Linda Feldmann, Albert Saiz, Markus Reindl, Patrice H. Lalive, Claude C. Bernard, Wolfgang Brück, and Martin S. Weber. 2016. 'Myelin-reactive antibodies initiate T cell-mediated CNS autoimmune disease by opsonization of endogenous antigen', *Acta Neuropathol.*, 132: 43-58.
- Koch, M, M Pancera, PD Kwong, P Kolchinsky, C Grundner, L Wang, WA Hendrickson, J Sodroski, and R Wyatt. 2003. 'Structure-based, targeted deglycosylation of HIV-1 gp120 and effects on neutralization sensitivity and antibody recognition.', *Virology.*, 313: 387-400.
- Krumbholz, Markus, and Edgar Meinl. 2014. 'B cells in MS and NMO: pathogenesis and therapy', *Semin Immunopathol.*, 36: 339-50.
- Kutzelnigg, A, i C Lucchinetti, C Stadelmann, W Brück, H Rauschka, M Bergmann, M Schmidbauer, J Parisi, and H Lassmann. 2005. 'Cortical demyelination and diffuse white matter injury in multiple sclerosis', *Brain*, 128: 2705-12.
- Labasque, Marilyne, Bruno Hivert, Gisela Nogales-Gadea, Luis Querol, Isabel Illa, and Catherine Faivre-Sarrailh. 2014. 'Specific Contactin N -Glycans Are Implicated in Neurofascin Binding and Autoimmune Targeting in Peripheral Neuropathies', *J Biol Chem.*, 289: 7907-18.
- Lee, CH, G Romain, W Yan, M Watanabe, W Charab, B Todorova, J Lee, K Triplett, M Donkor, OI Lungu, A Lux, N Marshall, MA Lindorfer, OR Goff, B Balbino, TH Kang, H Tanno, G Delidakis, C Alford, RP Taylor, F Nimmerjahn, N Varadarajan, P Bruhns, YJ Zhang, and G Georgiou. 2017. 'IgG Fc domains that bind C1q but not effector Fcγ receptors delineate the importance of complement-mediated effector functions.', *Nat Immunol*: 889-98.
- Lennon, VA, DM Wingerchuk, TJ Kryzer, SJ Pittock, CF Lucchinetti, K Fujihara, I Nakashima, and BG Weinshenker. 2004. 'A serum autoantibody marker of neuromyelitis optica: distinction from multiple sclerosis.', *Lancet*, 364: 2106-12.
- Lennon, Vanda A., Thomas J. Kryzer, Sean J. Pittock, A. S. Verkman, and Shannon R. Hinson. 2005. 'IgG marker of optic-spinal multiple sclerosis binds to the aquaporin-4 water channel', *J Exp Med.*, 202: 473-77.
- Linnington, C, and H Lassmann. 1987. 'Antibody responses in chronic relapsing experimental allergic encephalomyelitis: correlation of serum demyelinating activity with antibody titre to the myelin oligodendrocyte glycoprotein (MOG)', *J Neuroimmunol*, 17: 61-69.
- Litzenburger, T, R Fässler, J Bauer, H Lassmann, C Linnington, H Wekerle, and A Iglesias. 1998. 'B lymphocytes producing demyelinating autoantibodies: development and function in gene-targeted transgenic mice', *J Exp Med*, 188: 169-80.
- Lock, C, G Hermans, R Pedotti, A Brendolan, E Schadt, H Garren, A Langer-Gould, S Strober, B Cannella, J Allard, Klonowskis P, A Austin, N Lad, N Kaminski, SJ Galli, JR Oksenberg, CS Raine, R Heller, and L Steinman. 2002. 'Gene-microarray analysis of multiple sclerosis lesions yields new targets validated in autoimmune encephalomyelitis', *Nat Med.*, 8: 500-08.
- Lucchinetti, C, W Brück, J Parisi, B Scheithauer, M Rodriguez, and H Lassmann. 2000. 'Heterogeneity of multiple sclerosis lesions: implications for the pathogenesis of demyelination.', *Ann Neurol.*, 47: 707-17.
- Lucchinetti, CF, RN Mandler, D McGavern, W Bruck, G Gleich, RM Ransohoff, C Trebst, B Weinshenker, D Wingerchuk, JE Parisi, and H Lassmann. 2002. 'A role for humoral mechanisms in the pathogenesis of Devic's neuromyelitis optica.', *Brain*, 127: 1450-61.

- Macauley, M. S., P. R. Crocker, and J. C. Paulson. 2014. 'Siglec-mediated regulation of immune cell function in disease', *Nat Rev Immunol*, 14: 653-66.
- Mader, Simone, Viktoria Gredler, Kathrin Schanda, Kevin Rostasy, Irena Dujmovic, Kristian Pfaller, Andreas Lutterotti, Sven Jarius, Franziska Di Pauli, Bettina Kuenz, Rainer Ehling, Harald Hegen, Florian Deisenhammer, Fahmy Aboul-Enein, Maria K. Storch, Peter Koson, Jelena Drulovic, Wolfgang Kristoferitsch, Thomas Berger, and Markus Reindl. 2011. 'Complement activating antibodies to myelin oligodendrocyte glycoprotein in neuromyelitis optica and related disorders', *J Neuroimmunol*, 8: 184.
- Malik, R., T. Dau, M. Gonik, A. Sivakumar, D. J. Deredge, E. V. Edeleva, J. Gotzfried, S. W. van der Laan, G. Pasterkamp, N. Beaufort, S. Seixas, S. Bevan, L. F. Lincz, E. G. Holliday, A. I. Burgess, K. Rannikmae, J. Minnerup, J. Kriebel, M. Waldenberger, M. Muller-Nurasyid, P. Lichtner, D. Saleheen, P. M. Rothwell, C. Levi, J. Attia, C. L. Sudlow, D. Braun, H. S. Markus, P. L. Wintrode, K. Berger, D. E. Jenne, and M. Dichgans. 2017. 'Common coding variant in SERPINA1 increases the risk for large artery stroke', *Proc Natl Acad Sci U S A*, 114: 3613-18.
- Marti Fernandez, I, C Macrini, M Krumbholz, PJ Hensbergen, AL Hipgrave Ederveen, S Winklmeier, A Vural, A Kurne, D Jenne, F Kamp, LA Gerdes, R Hohlfeld, M Wuhrer, T Kümpfel, and E Meinl. 2019. 'The Glycosylation Site of Myelin Oligodendrocyte Glycoprotein Affects Autoantibody Recognition in a Large Proportion of Patients', *Front Immunol*, 10: 1189.
- Mayer, M. C., C. Breithaupt, M. Reindl, K. Schanda, K. Rostasy, T. Berger, R. C. Dale, F. Brilot, T. Olsson, D. Jenne, A. K. Probstel, K. Dornmair, H. Wekerle, R. Hohlfeld, B. Banwell, A. Bar-Or, and E. Meinl. 2013. 'Distinction and Temporal Stability of Conformational Epitopes on Myelin Oligodendrocyte Glycoprotein Recognized by Patients with Different Inflammatory Central Nervous System Diseases', *J Immunol.*, 191: 3594-604.
- Mayer, M. C., and E. Meinl. 2012. 'Glycoproteins as targets of autoantibodies in CNS inflammation: MOG and more', *Ther Adv Neurol Disord.*, 5: 147-59.
- McLaughlin, K. A., T. Chitnis, J. Newcombe, B. Franz, J. Kennedy, S. McArdel, J. Kuhle, L. Kappos, K. Rostasy, D. Pohl, D. Gagne, J. M. Ness, S. Tenenbaum, K. C. O'Connor, V. Vigiotta, S. J. Wong, N. P. Tavakoli, J. De Seze, Z. Idrissova, S. J. Khoury, A. Bar-Or, D. A. Hafler, B. Banwell, and K. W. Wucherpfennig. 2009. 'Age-Dependent B Cell Autoimmunity to a Myelin Surface Antigen in Pediatric Multiple Sclerosis', *J Immunol.*, 183: 4067-76.
- Merle, Nicolas S., Sarah Elizabeth Church, Veronique Fremeaux-Bacchi, and Lubka T. Roumenina. 2015. 'Complement System Part I – Molecular Mechanisms of Activation and Regulation', *Front Immunol*, 6: 262.
- Misu, Tatsuro, Romana Höftberger, Kazuo Fujihara, Isabella Wimmer, Yoshiki Takai, Shuhei Nishiyama, Ichiro Nakashima, Hidehiko Konno, Monika Bradl, Ferenc Garzuly, Yasuto Itoyama, Masashi Aoki, and Hans Lassmann. 2013. 'Presence of six different lesion types suggests diverse mechanisms of tissue injury in neuromyelitis optica', *Acta Neuropathol.*, 125: 815-27.
- Montalban, Xavier, Stephen L. Hauser, Ludwig Kappos, Douglas L. Arnold, Amit Bar-Or, Giancarlo Comi, Jérôme De Seze, Gavin Giovannoni, Hans-Peter Hartung, Bernhard Hemmer, Fred Lublin, Kottil W. Rammohan, Krzysztof Selmaj, Anthony Traboulsee, Annette Sauter, Donna Masterman, Paulo Fontoura, Shibeshih Belachew, Hideki Garren, Nicole Mairon, Peter Chin, and Jerry S. Wolinsky. 2017. 'Ocrelizumab versus Placebo in Primary Progressive Multiple Sclerosis', *New England Journal of Medicine*, 376: 209-20.
- Niederfellner, G., A. Lammens, O. Mundigl, G. J. Georges, W. Schaefer, M. Schwaiger, A. Franke, K. Wiechmann, S. Jenewein, J. W. Slootstra, P. Timmerman, A. Brannstrom, F. Lindstrom, E. Mossner, P. Umana, K. P. Hopfner, and C. Klein. 2011. 'Epitope

- characterization and crystal structure of GA101 provide insights into the molecular basis for type I/II distinction of CD20 antibodies', *Blood.*, 118: 358-67.
- Nimmerjahn, Falk, and Jeffrey V. Ravetch. 2008. 'Fcγ receptors as regulators of immune responses', *Nat Rev Immunol*, 8: 34.
- O'Connor, Kevin C., Katherine A. McLaughlin, Philip L. De Jager, Tanuja Chitnis, Estelle Bettelli, Chenqi Xu, William H. Robinson, Sunil V. Cherry, Amit Bar-Or, Brenda Banwell, Hikoaki Fukaura, Toshiyuki Fukazawa, Silvia Tenembaum, Susan J. Wong, Norma P. Tavakoli, Zhannat Idrissova, Vissia Viglietta, Kevin Rostasy, Daniela Pohl, Russell C. Dale, Mark Freedman, Lawrence Steinman, Guy J. Buckle, Vijay K. Kuchroo, David A. Hafler, and Kai W. Wucherpfennig. 2007. 'Self-antigen tetramers discriminate between myelin autoantibodies to native or denatured protein', *Nat Med.*, 13: 211-17.
- Obermeier, Birgit, Reinhard Mentele, Joachim Malotka, Josef Kellermann, Tania Kümpfel, Hartmut Wekerle, Friedrich Lottspeich, Reinhard Hohlfeld, and Klaus Dornmair. 2008. 'Matching of oligoclonal immunoglobulin transcriptomes and proteomes of cerebrospinal fluid in multiple sclerosis', *Nat Med.*, 14: 688-93.
- Pellkofer, H. L., M. Krumbholz, A. Berthele, B. Hemmer, L. A. Gerdes, J. Havla, R. Bittner, M. Canis, E. Meinl, R. Hohlfeld, and T. Kuempfel. 2011. 'Long-term follow-up of patients with neuromyelitis optica after repeated therapy with rituximab', *Neurology.*, 76: 1310-15.
- Perera, N. C., O. Schilling, H. Kittel, W. Back, E. Kremmer, and D. E. Jenne. 2012. 'NSP4, an elastase-related protease in human neutrophils with arginine specificity', *Proc Natl Acad Sci USA*, 109: 6229-34.
- Pham-Dinh, D, MG Mattei, JL Nussbaum, G Roussel, P Pontarotti, N Roedel, IH Mather, K Artzt, KF Lindahl, and A Dautigny. 1993. 'Myelin/oligodendrocyte glycoprotein is a member of a subset of the immunoglobulin superfamily encoded within the major histocompatibility complex.', *Proc Natl Acad Sci U S A.*, 90: 7990-4.
- Phuan, PW, J Ratelade, A Rossi, L Tradtrantip, and AS Verkman. 2012. 'Complement-dependent cytotoxicity in neuromyelitis optica requires aquaporin-4 protein assembly in orthogonal arrays.', *J Biol Chem.*, 287: 13829-39.
- Piddlesden, SJ, H Lassmann, F Zimprich, BP Morgan, and C Linington. 1993. 'Piddlesden SJ1, Lassmann H, Zimprich F, Morgan BP, Linington C.', *Am J Pathol.*, 143: 555-64.
- Pröbstel, AK, K Dornmair, R Bittner, P Sperl, D Jenne, S Magalhaes, A Villalobos, C Breithaupt, R Weissert, U Jacob, M Krumbholz, T Kuempfel, A Blaschek, W Stark, J Gärtner, D Pohl, K Rostasy, F Weber, I Forne, M Khademi, T Olsson, F Brilot, E Tantsis, RC Dale, H Wekerle, R Hohlfeld, B Banwell, A Bar-Or, E Meinl, and T Derfuss. 2011. 'Antibodies to MOG are transient in childhood acute disseminated encephalomyelitis.', *Neurology*, 77: 580-8.
- Quast, I, and JD Lünemann. 2014. 'Fc glycan-modulated immunoglobulin G effector functions.', *J Clin Immunol.*, 34: S51-5.
- Ratelade, Julien, Nithi Asavapanumas, Alanna M. Ritchie, Scott Wemlinger, Jeffrey L. Bennett, and A. S. Verkman. 2013. 'Involvement of antibody-dependent cell-mediated cytotoxicity in inflammatory demyelination in a mouse model of neuromyelitis optica', *Acta Neuropathologica*, 126: 699-709.
- Reindl, M, F Di Pauli, K Rostásy, and T Berger. 2013. 'The spectrum of MOG autoantibody-associated demyelinating diseases.', *Nat Rev Neurol.*: 455-61.
- Reindl, Markus, and Patrick Waters. 2019. 'Myelin oligodendrocyte glycoprotein antibodies in neurological disease', *Nat Rev Neurol.*, 15: 89-102.
- Reitter, J. N., R. E. Means, and R. C. Desrosiers. 1998. 'A role for carbohydrates in immune evasion in AIDS', *Nat Med*, 4: 679-84.
- Russell, Alyce, Eric Adua, Ivo Ugrina, Simon Laws, and Wei Wang. 2018. 'Unravelling Immunoglobulin G Fc N-Glycosylation: A Dynamic Marker Potentiating Predictive, Preventive and Personalised Medicine', *Int J Mol Sci*, 19: 390.

- Saadoun, Samira, Patrick Waters, Gregory P. Owens, Jeffrey L. Bennett, Angela Vincent, and Marios C. Papadopoulos. 2014. 'Neuromyelitis optica MOG-IgG causes reversible lesions in mouse brain', *Acta Neuropathol Commun.*, 2: 35.
- Sadovnick, AD, and GC Ebers. 1993. 'Epidemiology of multiple sclerosis: a critical overview.', *Can J Neurol Sci*, 20: 17-29.
- Schluesener, HJ, RA Sobel, C Lington, and HL Weiner. 1987. 'A monoclonal antibody against a myelin oligodendrocyte glycoprotein induces relapses and demyelination in central nervous system autoimmune disease.', *J Immunol.*, 139: 4016-21.
- Shields, R. L., A. K. Namenuk, K. Hong, Y. G. Meng, J. Rae, J. Briggs, D. Xie, J. Lai, A. Stadlen, B. Li, J. A. Fox, and L. G. Presta. 2001. 'High Resolution Mapping of the Binding Site on Human IgG1 for FcγRI, FcγRII, FcγRIII, and FcRn and Design of IgG1 Variants with Improved Binding to the FcγRI', *J Biol Chem.*, 276: 6591-604.
- Sorensen, P. S., S. Lisby, R. Grove, F. Derosier, S. Shackelford, E. Havrdova, J. Drulovic, and M. Filippi. 2014. 'Safety and efficacy of ofatumumab in relapsing-remitting multiple sclerosis: A phase 2 study', *Neurology.*, 82: 573-81.
- Spadaro, Melania, Lisa Ann Gerdes, Markus Krumbholz, Birgit Ertl-Wagner, Franziska Sabrina Thaler, Elisabeth Schuh, Imke Metz, Astrid Blaschek, Andrea Dick, Wolfgang Brück, Reinhard Hohlfeld, Edgar Meinl, and Tania Kümpfel. 2016. 'Autoantibodies to MOG in a distinct subgroup of adult multiple sclerosis', *Neurol Neuroimmunol Neuroinflamm.*, 3: e257.
- Spadaro, Melania, Lisa Ann Gerdes, Marie C. Mayer, Birgit Ertl-Wagner, Sarah Laurent, Markus Krumbholz, Constanze Breithaupt, Tobias Högen, Andreas Straube, Armin Giese, Reinhard Hohlfeld, Hans Lassmann, Edgar Meinl, and Tania Kümpfel. 2015. 'Histopathology and clinical course of MOG-antibody-associated encephalomyelitis', *Ann Clin Transl Neurol.*, 2: 295-301.
- Spadaro, Melania, Stephan Winklmeier, Eduardo Beltrán, Caterina Macrini, Romana Höftberger, Elisabeth Schuh, Franziska S. Thaler, Lisa Ann Gerdes, Sarah Laurent, Ramona Gerhards, Simone Brändle, Klaus Dornmair, Constanze Breithaupt, Markus Krumbholz, Markus Moser, Gurumoorthy Krishnamoorthy, Frits Kamp, Dieter Jenne, Reinhard Hohlfeld, Tania Kümpfel, Hans Lassmann, Naoto Kawakami, and Edgar Meinl. 2018. 'Pathogenicity of human antibodies against myelin oligodendrocyte glycoprotein', *Annals of Neurology*, 84: 315-28.
- Tao, MH, RI Smith, and SL Morrison. 1993. 'Structural features of human immunoglobulin G that determine isotype-specific differences in complement activation.', *J Exp Med.*, 178: 661-7.
- Tatomir, Alexandru, Anamaria Talpos-Caia, Freidrich Anselmo, Adam M. Kruszewski, Dallas Boodhoo, Violeta Rus, and Horea Rus. 2017. 'The complement system as a biomarker of disease activity and response to treatment in multiple sclerosis', *Immunol Res*, 65: 1103-09.
- Tenembaum, S., T. Chitnis, J. Ness, and J. S. Hahn. 2007. 'Acute disseminated encephalomyelitis', *Neurology.*, 68: S23-S36.
- Tradtrantip, L, H Zhang, S Saadoun, PW Phuan, C Lam, MC Papadopoulos, JL Bennett, and AS Verkman. 2012. 'Anti-aquaporin-4 monoclonal antibody blocker therapy for neuromyelitis optica.', *Ann Neurol.*, 71: 314-22.
- Trebst, Corinna, Sven Jarius, Achim Berthele, Friedemann Paul, Sven Schippling, Brigitte Wildemann, Nadja Borisow, Ingo Kleiter, Orhan Aktas, and Tania Kümpfel. 2014. 'Update on the diagnosis and treatment of neuromyelitis optica: Recommendations of the Neuromyelitis Optica Study Group (NEMOS)', *J Neurol.*, 261: 1-16.
- Ulvestad, E, K Williams, C Vedeler, J Antel, H Nyland, S Mørk, and R Matre. 1994. 'Reactive microglia in multiple sclerosis lesions have an increased expression of receptors for the Fc part of IgG.', *J Neurol Sci.*, 121: 125-31.

- Urich, E, I Gutcher, M Prinz, and B Becher. 2006. 'Autoantibody-mediated demyelination depends on complement activation but not activatory Fc-receptors.', *Proc Natl Acad Sci U S A.*, 103: 18697-702.
- Von Büdingen, Hans-Christian, Monica Gulati, Sandra Kuenzle, Katja Fischer, Tobias A. Rupprecht, and Norbert Goebels. 2010. 'Clonally expanded plasma cells in the cerebrospinal fluid of patients with central nervous system autoimmune demyelination produce "oligoclonal bands"', *J Neuroimmunol.*, 218: 134-39.
- Weber, MS, T Derfuss, I Metz, and Brück W. 2018. 'Defining distinct features of anti-MOG antibody associated central nervous system demyelination.', *Ther Adv Neurol Disord.*, Mar 29;11:1756286418762083.
- Wei, Xiping, Julie M. Decker, Shuyi Wang, Huxiong Hui, John C. Kappes, Xiaoyun Wu, Jesus F. Salazar-Gonzalez, Maria G. Salazar, J. Michael Kilby, Michael S. Saag, Natalia L. Komarova, Martin A. Nowak, Beatrice H. Hahn, Peter D. Kwong, and George M. Shaw. 2003. 'Antibody neutralization and escape by HIV-1', *Nature.*, 422: 307-12.
- Weinshenker, BG, B Bass, GP Rice, J Noseworthy, W Carriere, J Baskerville, and GC Ebers. 1989. 'The natural history of multiple sclerosis: a geographically based study. I. Clinical course and disability', *Brain*: 133–46.
- Weinshenker, BG, DM Wingerchuk, SJ Pittock, CF Lucchinetti, and VA Lennon. 2006. 'NMO-IgG: A specific biomarker for neuromyelitis optica', *Dis Markers*: 197–206.
- Wingerchuk, DM, VA Lennon, CF Lucchinetti, SJ Pittock, and BG Weinshenker. 2007. 'The spectrum of neuromyelitis optica', *Lancet Neurol*, 6: 805-15.
- Yogo, R, Y Yamaguchi, H Watanabe, H Yagi, T
- Nakanishi Satoh, M, M Onitsuka, T Omasa, M Shimada, T Maruno, T Torisu, S Watanabe, D Higo, T Uchihashi, S Yanaka, S Uchiyama, and K Kato. 2019. 'The Fab portion of immunoglobulin G contributes to its binding to Fcγ receptor III.', *Sci Rep*, 9(1).
- Zamvil, S. S., and A. J. Slavin. 2015. 'Does MOG Ig-positive AQP4-seronegative opticospinal inflammatory disease justify a diagnosis of NMO spectrum disorder?', *Neurol Neuroimmunol Neuroinflamm.*, 2: e62-e62.
- Zhou, D., R. Srivastava, S. Nessler, V. Grummel, N. Sommer, W. Bruck, H. P. Hartung, C. Stadelmann, and B. Hemmer. 2006. 'Identification of a pathogenic antibody response to native myelin oligodendrocyte glycoprotein in multiple sclerosis', *Proc Natl Acad Sci U S A.*, 103: 19057-62.
- Zielinska, Dorota F., Florian Gnad, Jacek R. Wiśniewski, and Matthias Mann. 2010. 'Precision Mapping of an In Vivo N-Glycoproteome Reveals Rigid Topological and Sequence Constraints', *Cell.*, 141: 897-907.

List of abbreviations

ADCC: antibody-dependent cell-mediated cytotoxicity

ADCP: antibody-dependent cell-mediated phagocytosis

ADEM: Acute disseminated encephalomyelitis

BON: Bilateral optic neuritis

CDC: Complement-dependent cytotoxicity

CDCC: Complement-dependent cell-mediated cytotoxicity

CDCP: Complement-dependent cell-mediated phagocytosis

CIS: Clinically isolated syndrome

CNS: Central nervous system

CSF: Cerebrospinal fluid

EAE: Experimental autoimmune encephalomyelitis

FcRs: Fc receptors

FcYR: Fc Y receptor

hMOG: human, wild-type MOG

IA: Immunoabsorption

LETM: Longitudinal extensive transverse myelitis

mAb: Monoclonal antibodies

MOG: Myelin oligodendrocyte glycoprotein

MRI: Magnetic resonance imaging

MS: Multiple sclerosis

Neu5Ac: N-acetylneuraminic acid

NGF: Nerve growth factor

NMOSD: Neuromyelitis optica spectrum disorders

OCB: Oligoclonal bands

ON: Optic neuritis

PPMS: Primary progressive multiple sclerosis

RON: Recurrent optic neuritis

RRMS: Relapsing-remitting multiple sclerosis

SIGLECS: Sialic acid-binding immunoglobulin like lectins

SPMS: Secondary progressive multiple sclerosis

TCC: Terminal complement complex

Publication and Conferences

Presentations:

Marti Fernandez I, Hensbergen P, Spadaro M, Hipgrave-Ederveen A, Gerdes L, Hohlfeld R, Kümpfel T, Huitinga I, Wuhrer M, Meinl E. Glycan structure of myelin oligodendrocyte glycoprotein (MOG) and its impact on autoantibody recognition. At the **11th International Congress on Autoimmunity** in Lisbon (May,2018) and at the **13th Dresden Symposium on Autoantibodies** in Dresden (September,2017)

Publication:

Marti Fernandez I, Macrini C, Krumbholz M, Hensbergen PJ, Hipgrave Ederveen AL, Winklmeier S, Vural A, Kurne A, Jenne D, Kamp F, Gerdes LA, Hohlfeld R, Wuhrer M, Kümpfel T and Meinl E. 2019. '*The glycosylation site of myelin oligodendrocyte glycoprotein affects autoantibody recognition in a large proportion of patients*'. Front Immunol, 10:1189.